OAK RIDGE
NATIONAL LABORATORY
MANAGED BY UT-BATTELLE
FOR THE DEPARTMENT OF ENERGY

ORNL/SUB/99-B99398V-6

Spatial Kinetics Calculations of MOX Fuelled Core: Variant 22

A. M. Pavlovichev
S. N. Bolshagin
A. A. Pinegin
L. K. Shishkov
D. L. Shishkov
B. E. Shumsky
Y. A. Styrin

Fissile Materials Disposition Program

UT-BATTELLE
ORNL-27 (4-00)

DOCUMENT AVAILABILITY

Reports produced after January 1, 1996, are generally available free via the U.S. Department of Energy (DOE) Information Bridge.

Web site http://www.osti.gov/bridge

Reports produced before January 1, 1996, may be purchased by members of the public from the following source.

National Technical Information Service
5285 Port Royal Road
Springfield, VA 22161
Telephone 703-605-6000 (1-800-553-6847)
TDD 703-487-4639
Fax 703-605-6900
E-mail info@ntis.fedworld.gov
Web site http://www.ntis.gov/support/ordernowabout.htm

Reports are available to DOE employees, DOE contractors, Energy Technology Data Exchange (ETDE) representatives, and International Nuclear Information System (INIS) representatives from the following source.

Office of Scientific and Technical Information
P.O. Box 62
Oak Ridge, TN 37831
Telephone 865-576-8401
Fax 865-576-5728
E-mail reports@adonis.osti.gov
Web site http://www.osti.gov/contact.html

This report was prepared as an account of work sponsored by an agency of the United States Government. Neither the United States Government nor any agency thereof, nor any of their employees, makes any warranty, express or implied, or assumes any legal liability or responsibility for the accuracy, completeness, or usefulness of any information, apparatus, product, or process disclosed, or represents that its use would not infringe privately owned rights. Reference herein to any specific commercial product, process, or service by trade name, trademark, manufacturer, or otherwise, does not necessarily constitute or imply its endorsement, recommendation, or favoring by the United States Government or any agency thereof. The views and opinions of authors expressed herein do not necessarily state or reflect those of the United States Government or any agency thereof.

ORNL/SUB/99-B99398V-6

SPATIAL KINETICS CALCULATIONS OF MOX FUELLED CORE: VARIANT 22

A. M. Pavlovichev
S. N. Bolshagin
A. A. Pinegin
L. K. Shishkov
D. L. Shishkov
B. E. Shumsky
Y. A. Styrin

Date Published: December 2000

Prepared by
Russian Research Center "Kurchatov Institute"
Institute of Nuclear Reactors
under subcontract 85B-99398V

Funded by
Office of Fissile Materials Disposition
U.S. Department of Energy

Prepared for
Computational Physics and Engineering Division
OAK RIDGE NATIONAL LABORATORY
Oak Ridge, Tennessee 37831
managed by
UT-BATTELLE, LLC
for the
U.S. DEPARTMENT OF ENERGY
under contract DE-AC05-00OR22725

Page Intentionally Blank

Russian Research Center "Kurchatov Institute"
Institute of Nuclear Reactors
VVER Division

Joint U.S. / Russian Project to Update, Verify and Validate Reactor Design/Safety Computer Codes Associated with Weapons-Grade Plutonium Disposition in VVER Reactors

Spatial Kinetics Calculations of MOX Fuelled Core. Variant 22

(Report)

General Order 85B-99398V. Work Release 02. P. 99-4a

Project Manager

A.M.Pavlovichev

Executed by

S.N.Bolshagin
A.A.Pinegin
L.K.Shishkov
D.L.Shishkov
B.E.Shumsky
Y.A.Styrin

Moscow 1999

ACRONYMS

Russian		West Equivalent
AZ	emergency (accident) protection	AP
AZ-1	state with all the control rods fully inserted except of one the most effective stuck in upper position	AP-1
BOC	Beginning Of fuel Cycle	BOC
BPR	Burnable Poison Rod	BPR
BRU-A	Atmospheric Steam Dump (PG Relief Valves)	
DNB	Departure from Nucleate Boiling (passing of Critical Heat Flux)	DNB
DNBR	Departure from Nucleate Boiling Ratio	DNBR
DTC	Doppler Temperature Coefficient	DTC
EFPD	Effective Full Power Day	EFPD
EOC	End Of fuel Cycle	EOC
FP	Fission Products	FP
KI	Kurchatov Institute	KI
LTA	Lead Test Assembly	LTA
LWR	Light Water Reactor	LWR
MCL	Minimum Controllable reactor power Level	MCL
MDC	Moderator Density Coefficient	MDC
MOX	Mixed Oxide (uranium-plutonium fuel)	MOX
MTC	Moderator Temperature Coefficient	MTC
NPP	Nuclear Power Plant	NPP
OR	Regulatory Body (Control Rod)	CR
PG	Steam Generator	SG
PWR	Pressurized-Water Reactor	PWR
RCT	Repeat Criticality Temperature	RCT
SUZ	Reactor Control and Protection System	RPS
TVS, FA	Fuel Assembly	FA
UOX, LEU	Uranium Oxide Fuel (Light Enrichment Uranium)	UOX, LEU
VVER	Russian water-water reactor	VVER

Executive Summary

In this document the reactor-kinetics benchmarks are presented for 30% MOX fuelled core of VVER-1000. Both UOX and MOX cores are calculated for three types of accidents:

- control rod ejection,
- overcooling of the reactor core caused by steam line rupture,
- boron dilution of coolant.

CONTENTS

INTRODUCTION 6
1. Brief Description of Code NOSTRA 7
2. Definitions 9
3. Equilibrium Fuel Cycle with 30% MOX Loaded Core (Variant 21) 14
4. Central Control Rod Ejection from the VVER-1000 Core 38
5. Core Cooling in Case of Steam Line Rupture 48
6. The Boron Dilution of Coolant in a Part of the VVER-1000 Core 57
CONCLUSION 68
REFERENCE 69

Table 3-1. Composition of Weapons Grade Plutonium 15
Table 3-2. Main Core Parameters 15
Table 3-3. Fuel Assembly Design Parameters 16
Table 3-4. Uranium Fuel Pin Design Parameters 17
Table 3-5. MOX Fuel Pin Design Parameters 18
Table 3-6. Discrete Burnable Poison Pin Design Parameters 19
Table 3-7. Control Rod Design Parameters 20
Table 5-1. Accident sequence 48
Table 5-2. Variation of Core Parameters in the Accident with Steam Line Rupture and Power Unit de-Energized 49

Fig. 3-1. Simplified Design for 3 Zones MOX LTA 21
Fig. 3-2. Simplified Design for VVER-1000 Fuel Assembly. Type A 22
Fig. 3-3. Simplified Design for VVER-1000 Fuel Assembly. Type B, Ba and Bb 23
Fig. 3-4. Simplified Design for VVER-1000 Fuel Assembly. Type C 24
Fig. 3-5. Equilibrium Loading Pattern for Base Uranium Core with Boron BPRs 25
Fig. 3-6. Uranium Zone. Assembly Burnup, Relative Power 26
Fig. 3-7. Equilibrium Loading Pattern for MOX Fuelled Core with 54 MOX Fuel Assemblies 27
Fig. 3-8. MOX Zone. Assembly Burnup, Relative Power. 28
Fig. 3-9. Control Rods Grouping and Positions of In-core Self-Powered Detectors 29
Fig. 3-10. Assemblies Numeration in VVER-1000 Core 30
Fig. 3-11. Model of VVER-1000 Reflector 31
Fig. 3-12. Reflector "Assembly" of Type 1 32
Fig. 3-13. Reflector "Assembly" of Type 2 33
Fig. 3-14. Reflector "Assembly" of Type 3 34
Fig.3-17. Core Design. Material Contents (Vol%) in Axial Direction 37
Fig. 4-1. Uranium zone. Assembly burnup, relative power and temperature drop for control rod ejection calculation. 40
Fig. 4-2. MOX zone. Assembly burnup, relative power and temperature drop for control rod ejection calculation 41
Fig. 4-3. Reactivity. Central Control Rod Ejection 42
Fig. 4-4. Neutron Power. Central Control Rod Ejection 43

Fig. 4-5. Maximal Neutron Linear Power. Central Control Rod Ejection 44
Fig. 4-6. Maximal Fuel Temperature. Central Control Rod Ejection 45
Fig. 4-7. Minimal DNBR. Central Control Rod Ejection 46
Fig. 4-8. Maximal Fuel Enthalpy. Central Control Rod Ejection 47
Fig. 5-1. Inlet Temperature in Different Parts of the Core. Partial Core Overcooling . 50
Fig. 5-2. Reactivity. Partial Core Overcooling 51
Fig. 5-3. Neutron Power. Partial Core Overcooling 52
Fig. 5-4. Maximal Neutron Linear Power. Partial Core Overcooling 53
Fig. 5-5. Maximal Fuel Temperature. Partial Core Overcooling 54
Fig. 5-6. Minimal DNBR. Partial Core Overcooling 55
Fig. 5-7. Assembly Power. Partial Core Overcooling. MOX + LEU 56
Fig. 6-1. Numbers of Fuel Assemblies in the Quarter of the Core 59
Fig. 6-2. Concentration of Boron Acid. Loop Put into Operation & Boron Dilution ... 60
Fig. 6-3. Reactivity. Loop Put into Operation & Boron Dilution 61
Fig. 6-4. Neutron Power. Loop Put into Operation & Boron Dilution 62
Fig. 6-5. Maximal Neutron Power. Loop Put into Operation & Boron Dilution 63
Fig. 6-6. Maximal Fuel Temperature. Loop Put into Operation & Boron Dilution 64
Fig. 6-7. Minimal DNBR. Loop Put into Operation & Boron Dilution 65
Fig. 6-8. Maximal Fuel Enthalpy. Loop Put into Operation & Boron Dilution 66
Fig. 6-9. Power of Assembly N 4. Loop Put into Operation & Boron Dilution 67

INTRODUCTION

This work is a part of Joint U.S. / Russian Project with Weapons-Grade Plutonium Disposition in VVER Reactors and presents the results of spatial kinetics calculational benchmarks.

The examinations were carried out with the following purposes:

- to verify one of spatial neutronic kinetics model elaborated in KI,
- to understand sensibility of the model to neutronics difference of UOX and MOX cores,
- to compare in future point and spatial kinetics models (on the base of a set of selected accidents) in view of eventual creation of RELAP option with 3D kinetics.

The document contains input data and results of model operation of three emergency dynamic processes in the VVER-1000 core:

- Central control rod ejection by pressure drop caused by destroying of the moving mechanism cover.
- Overcooling of the reactor core caused by steam line rupture and non-closure of steam generator stop valve.
- The boron dilution of coolant in part of the VVER-1000 core caused by penetration of the distillate slug into the core at start up of non-working loop.

These accidents have been applied to

- Uranium reference core that is the so-called Advanced VVER-1000 core with Zirconium fuel pins claddings and guide tubes. A number of assemblies contained 18 boron BPRs while first year operating.
- MOX core with about 30% MOX fuel.

At a solving it was supposed that MOX-fuel thermophysical characteristics are identical to uranium fuel ones.

The calculations were carried out with the help of the program NOSTRA / 1 /, simulating VVER dynamics that is briefly described in Chapter1.

Chapter 3 contains the description of reference Uranium and MOX cores that are used in calculations. The neutronics calculations of MOX core with about 30% MOX fuel are named "Variant 21".

Chapters 4-6 contain the calculational results of three above mentioned benchmark accidents that compose in a whole the "Variant 22".

1. Brief Description of Code NOSTRA

Code NOSTRA have been developed for safety parameters investigations of nuclear power plants (NPP) with reactors of VVER type. Code is intended for computational analysis of transient and accidental processes that may include arising of core multiplying properties ingomogeneity, for example failures of steam generator operation due to non-complete mixing of coolant in pressure chamber, "shooting" of alone cluster etc.

Code NOSTRA allows to obtain the time-dependent three-dimensional neutron and temperature distributions in core. Code is capable to model the variations of NPP equipment operation regime for known time-dependencies of flow rate, pressure and temperature of coolant at the core inlet and for known strategy of control rods movement.

Code allows to compute the transient and accidental regimes caused by the following reasons:

- failures of main circulation pumps;
- variation in steam generator load;
- failures in feed water system;
- rupture of pipelines in the 2-nd circuit;
- rupture of pipelines in feed water system;
- rupture of pipelines in auxiliary system of the 1-st circuit;
- action of reactor power control system;
- violation in action of reactor power control system, e.g. self-movement of control rod, sticking of cluster during operation etc.;
- throwing out the cluster;
- any combination of these reasons.

Code is capable to perform the operational computations for NPP with reactors VVER-440, VVER-1000 and design computations for advanced NPPs.

Neutronics processes are simulated on the basis of certified code BIPR-7 [2] methodology that was generalized on non-stationary equations with 6 groups of delayed neutron predecessors and non zero life-time of prompt neutrons. Code BIPR-7 considers 3-dimensional 1.5-group diffusion model of neutron transport. Diffusion equations are solved by the 'coarse-mesh' method with coefficients obtained with using of nodal algorithm. Asymptotic and transient functions of each node are utilized as modes. Additional balances are formed at the boundaries of considered prisms. Algorithm takes into account the discontinuity of diffusion properties on boundaries of nodes. For solving of the algebraic equations the non-linear iterative procedure is used that permits to reduce the dimensionality of the problem.

Neutronics characteristics of nodes are approximated by polynomials depending on the sort of fuel, fuel burnup, concentrations of boron and xenon, temperature distribution and state of coolant. The applicability of neutron algorithms is restricted to the steam content of no more than 10%.

Code solves the burnup equations and permit to analyse transients in any time of reactor operation. Model of residual heat generation takes into account the fuel burnup and is based on US Standard ANS-5.1.

Fuel and coolant temperature, concentrations of delayed neutrons predecessors are defined as average values for considered prisms formed in core space discretization as in codes of BIPR type.

Thermophysical model of the fuel elements considers the cladding, gas-gap and three fuel layers. Equations of heat and mass transfer are solved by explicit-implicit methods. Choice of method depends on the value of time step. Hydraulic computation is carried out for each assembly allowing to consider the situations with increased hydraulic resistance of some assemblies.

Code NOSTRA is provided by special system for graphic and tabular presentation of output data. Particularly, there is a capability to print two- and three-dimensional histograms of temperature and neutron fields. Code NOSTRA is forming the files of three-dimensional neutron fields for each step of time. It is possible to perform the time scanning of reactor parameters as animated cartoon.

Calculational subroutines are written on FORTRAN-language, service subroutines - on PASCAL-language. Code NOSTRA is operated on computers of IBM PC type.

2. Definitions

Parameter	Abbreviation	Units	Remarks
Calculational system	CS		Multi-assembly or core
CS symmetry sector	Sim		30 for 30°, 60 for 60°, 120 for 120°, 360 for full CS.
Reactivity of CS	RO	pcm	RO = (Keff-1)/Keff*1.E5
Calculational volume	Vij		Axial fraction j of assembly number i. In VVER-1000 calculations, 10-30 axial fractions of equal volume are usually used.
Effective multiplication factor of CS	Keff		
Multiplication factor of CS	Ko		Relation of neutron generation to neutron absorption. For core calculations Ko values are attributed to Vij
3-D power distribution in core	q_{ij}		Power in Vij normalised by average Vij power
Volume power peaking factor	Kv		Maximum in q_{ij} values
Radial position of volume power peaking factor	N (Kv) or N_K		Number of assembly in calculational core sector where Kv is realised
Axial position of volume power peaking factor	M (Kv) or N_Z		Number of axial level where Kv is realised
3-D burnup distribution in core	BUij	MWd/kg or GWd/t	Burnup in Vij.
2-D power distribution in core	q_i		Assembly powers normalised by average assembly power in core.
Radial power peaking factor	Kq		Maximum in qi values
Radial position of radial power peaking factor	N (Kq) or N_K		Number of assembly in calculational core sector where Kq is realised
Pin linear power	Ql	W/cm	Pin power for 1 cm of an axial calculational fraction
Moment during fuel irradiation	T	EFPD	

2-D burnup distribution in core	BUi	MWd/kg	Average-assembly burnup distribution in core.
Average burnup in Uranium assemblies	$\bar{B}_U$	MWd/kg or GWd/t	
Average burnup in MOX assemblies	$\bar{B}_{MOX}$	MWd/kg or GWd/t	
Average Boron acid (H_3BO_3) concentration[a] in coolant	Cb or C_{H3BO3}	ppm or g/kg	H_3BO_3 fraction in coolant (unit "ppm" means mg of boron acid in 1 Kg of H_2O)
Critical boron acid concentration in coolant	Cb^{crit}	ppm or g/kg	Cb (C_{H3BO3}) value ensuring Keff=1
2-D power distribution in CS	q_k-CS		Power of fuel pins normalised by average fuel pin power in CS.
Peaking factor of 2-D power distribution in CS	K_{FA}–CS		Maximum in q_k-CS values
2-D power distribution in assembly	q_k		Power of fuel pins normalised by average fuel pin power in assembly (in some axial fraction).
3-D power distribution in axial volumes of fuel pins in core	q_{ijk}		Power of axial volumes of fuel pins normalised by average power in such volumes over a whole core
Pin power peaking factor in assembly	Kki		Among q_k values for an assembly number i for a fraction number j where maximum q_{ij} for this assembly is realised.
Radial pin power peaking factor	Kr		max (qi * Kki)
Radial position of radial pin power peaking factor	N (Kr) or N_K		Number of assembly in calculational core sector where Kr is realised
2-D power peaking factor in assembly	K_{FA} (notation Kk or Kk_{max} is also used)		Maximum relative power of fuel pins (maximum in q_k values)

[a] Boron acid concentration divided by the coefficient 5.72 means natural boron (nat B) concentration. In VVER-1000 calculations the term of boron acid concentration is widely used. Below, Cb means boron acid concentration if there is no special indication.

Axial power peaking factor in assembly or in fuel pin	Kz		Maximum relative power of axial volume in assembly or in fuel pin normalised by average power in such volumes (in assembly or in fuel pin)
Total power peaking factor	Ko or $K_{o\text{-}total}$		$\max_{ij} (q_{ij} * Kki) = Kr*Kz$
Radial position of total power peaking factor	N ($K_{o\text{-}total}$) or N_K		Number of assembly in calculational core sector where $K_{o\text{-}total}$ is realised
Axial position of total power peaking factor	M ($K_{o\text{-}total}$) or N_Z		Number of axial level where $K_{o\text{-}total}$ is realised
Engineering factor	K_{eng}		Coefficient taking account of uncertainty of a hot point (maximum fuel pin local power) calculations
2-D burnup distribution in assembly	BUk	MWd/kg or GWd/t	Average-pin burnup distribution in CS.
1-D burnup distribution in fuel pin	BUpin		Burnup distribution in concentric zones of equal volume in fuel pin, normalised by average zone burnup.
1-D power distribution in fuel pin	q_{pin}		Power distribution in concentric zones of equal volume in fuel pin, normalised by average zone power.
Regulation bank position	H_{reg}	cm	Distance from core bottom till rods lower edge
Control rods worth (in core)	$(RO)_{AP\text{-}1}$	ppm	Effect of control rods insertion in core supposing the most effective single CR stuck in upper position. It is defined as a reactivity difference in two states: $(RO)_{AP\text{-}1}$= RO1-RO2. The second state differs from the first one only by additional CRs inserted in core. All the other

			parameters correspond to the first state: Cb (that is equal to Cb crit for the first state), temperature and FP distribution in core.
Repeat Criticality Temperature	RCT	°C	Temperature that ensures a secondary critical state during core cooling in EOC in such conditions: all control rods inserted in core except one the most effective, zero boron concentration, equilibrium xenon concentration corresponding to reactor power before its shut-down.
Moderator temperature coefficient (in core)	MTC	pcm/°C	
Moderator density coefficient (in core)	MDC	pcm/g/cc	
Doppler temperature coefficient (in core)	DTC	pcm/°C	Calculated supposing average fuel temperature changing of 1°C
Doppler isotermic temperature coefficient (in core)	DTC*	pcm/°C	Calculated supposing local fuel temperature changing of 1°C
Doppler power coefficient (in core)	DPC	pcm/MW	
Boron reactivity coefficient (in core)	DRO/DCB	pcm/ppm	
Effective fraction of delayed neutrons	βeff or $\beta_{ef.}$	ppm	General characteristic of infinite grid or core
Lifetime of prompt neutrons	l_m or l_{im}	s	General characteristic of infinite grid or core
Reactor thermal power	W	MW	
Specific reactor thermal power in CS	Wv	KW/litre	Reactor thermal power in CS volume unit
Nominal reactor thermal power	Wnom	MW	Equal to 3000 MW for VVER-1000
Minimum controllable level of reactor power	MCL	MW	In calculations corresponds to Zero Power and uniform temperature 280°C in core.
Core coolant flow rate	G	m^3/h	
Average entry core temperature	t_{entry}	°C or K	
Average outer core temperature	t_{out}	°C or K	
Average coolant-moderator temperature in CS	t_{mod}	°C or K	

Average Coolant-moderator density in CS	γ_{mod}	g/cm^3	
Fuel temperature	t_{fuel}	K	
Average temperature of other CS components	t_{con}	°C or K	
Fuel pin cladding temperature	t_{clad}	°C or K	
Xenon-135 concentration distribution in core	Xe	10^{24} /cc	For 1 cc in fuel. Xe = 0 → xenon is absent; Xe = 1 → Xe=Xe eq (W).
Equilibrium Xenon-135 concentration distribution in core	Xe eq (W)	10^{24} /cc	Concentration formed during long working with W power, regulating bank in nominal position[b]
Sm-149 concentration distribution in core	Sm	10^{24} /cc	For 1 cc in fuel. Sm = 0 → samarium is absent; Sm = 1 → Sm=Sm eq, Sm = 3 → full decay of Pm-149 into Sm-149 is simulated in BOC.
Equilibrium Sm-149 concentration distribution in core	Sm eq	10^{24} /cc	Concentration formed during long working, regulating bank in nominal position
Samarium-149 concentration distribution, all Prometium-149 decayed in Sm	Smh	10^{24} /cc	
Core reactivity while reactor shut-down	RO_{STOP}	pcm	Under conditions: W=0, Xe=0,Sm=Smh, t_{mod}= t_{fuel}= t_{con}=20°C, Cb= 16000 ppm

[b] In VVER-1000 calculations Hreg in nominal position is equal to 80% if there is no special indication

3. Equilibrium Fuel Cycle with 30% MOX Loaded Core (Variant 21)

Every accident calculation is to be executed for uranium reference core and for MOX fuelled core. The equilibrium fuel cycle of the "Uranium base core" with boron BPRs is presented in Figures 3-5 and 3-6. The simplified design of uranium fuel assemblies used here is shown in Figures 3-2, 3-3 and 3-4.

The first MOX core has been formed by introduction of 18 MOX assemblies into the uranium core periphery. The simplified design of MOX fuel assemblies is shown in Fig. 3-1. MOX fuel isotopic composition is presented in Table 3-1. The fissile plutonium enrichments are chosen, according to preliminary estimations, to ensure a reasonable value of pin power peaking factor in assembly. Equilibrium fuel cycle pattern of MOX fuelled core with 54 Plutonium assemblies is shown in Fig. 3-7 and Fig. 3-8. It is named "MOX core".

Characteristics of fuel rods, fuel assemblies, absorbers and boron poison rods are presented in Tables 3-2, 3-3, 3-4, 3-5, 3-6 and 3-7. Control rods grouping in VVER-1000 is presented in Fig. 3-9. The bank 10 is a regulating one inserted constantly into the core in the process of fuel irradiation. Assemblies' numeration is shown in Fig. 3-10.

The simplified structure of VVER-1000 radial reflector is presented in Fig. 3-11. In fine-mesh calculations that are carried out in KI the radial VVER-1000 reflector is modelled by "reflector assemblies" of five types (Figures 3-5, 3-12, 3-13, 3-14, 3-15 and 3-16). Zero flux is applied on the outer reflector borders.

Core modelling in axial direction is illustrated in Fig.3-17.

Fuel irradiation simulation is executed under the following conditions:

- The bank 10 is inserted of 20% core height all over a fuel cycle; the rest of banks are extracted;
- EOC corresponds to Cb crit =0;
- Equilibrium Sm and Xe;
- W = Wnom;
- t_{entry} = 287°C.

Table 3-1. Composition of Weapons Grade Plutonium

Isotope / content (W. %)				
Pu-238	Pu-239	Pu-240	Pu-241	Pu-242
0.0	93.0	6.0	1.0	0.0

Table 3-2. Main Core Parameters

Parameter	Units	Value
Thermal Power	MW thermal	3000
Electrical Power	MW	1000
Number of Coolant Loops		4
Number of Fuel Assemblies		163
Core Equivalent Diameter	m	3.164
Core Fuel Height	m	3.54
Core Volume	m^3	27.8
Core Power Density	W/cm^3	108
Control / Shut off Rod Banks		10
Position of Regulating Rod Bank	%	80
Reactor Coolant Flow Rate	m^3/hr	84000
Bypass Coolant Flow	%	3
Pressure at Core Inlet	MPa	16.1
Core Inlet Temperature	°C	287

Table 3-3. Fuel Assembly Design Parameters

Parameter	Units	Value
Shape of Fuel Assembly		Hexagonal
Distance Across Assembly (between flats)	cm	23.4
Distance Between Fuel Assembly Centres	cm	23.6
Fuel Pin Lattice Pitch	cm	1.275
Number of Fuel Pins in Fuel Assembly		312
Number of Guide Tubes for Control Rods / Burnable Absorber Pins		18
Inner Diameter of Guide Thimbles	cm	1.1
Thickness of Guide Thimbles	cm	0.1
Material of Guide Thimbles		Zirconium Alloy*
Central Instrumentation Tube Inner Diameter	cm	1.1
Thickness of Central Instrumentation Tube	cm	0.1
Material of Central Guide Tube		Zirconium Alloy *
Number of Spacer Grids in Fuel Assembly		13
Material of Spacer Grids		Zirconium Alloy*
Spacer Grid Weight (each)	Kg	0.55

Compositions Weight percent:

*

Zr	Nb	Hf
98.97	1.0	0.03

Table 3-4. Uranium Fuel Pin Design Parameters

Parameter	Units	Value
Inner Clad Diameter	cm	0.772
Clad Thickness	cm	0.069
Clad Material		Zirconium Alloy*
Clad Density	g / cc	6.5153
Fuel Pellet Diameter	cm	0.755
Central Hole Diameter	cm	0.15
Fuel Pellet Material		L.E. UO2
Height of Fuel Column	cm	353 (cold) 355 (hot)
Mass of UO2 in Fuel Pin	kg	1.575

Compositions Weight percent:

*

Zr	Nb	Hf
98.97	1.0	0.03

Table 3-5. MOX Fuel Pin Design Parameters

Parameter	Units	Value
Inner Clad Diameter	cm	0.772
Clad Thickness	cm	0.069
Clad Material		Zirconium Alloy*
Clad Density	g / cc	6.5153
Fuel Pellet Diameter	cm	0.755
Central Hole Diameter	cm	0.15
U-235 Content in MOX Fuel	%	0.2
Fuel Pellet Material		PuO2-UO2
Height of Fuel Column	cm	353 (cold) 355 (hot)
Mass of MOX Fuel in Fuel Pin	kg	1.600

Compositions Weight percent:

*

Zr	Nb	Hf
98.97	1.0	0.03

Table 3-6. Discrete Burnable Poison Pin Design Parameters

Parameter	Units	Value		
Clad Inner Diameter	cm	0.772		
Clad Thickness	cm	0.069		
Clad Material		Zirconium Alloy*		
Clad Density	g / cc	6.5153		
Absorber Diameter	cm	0.758		
Absorber Density	g / cc	2.869	2.896	2.945
Absorber Composition		Boron g / cc		
		0.020	0.036	0.065
B10	W%	0.1278	0.2279	0.4046
B11		0.5694	1.0153	1.8028
Al		93.5246	91.7424	88.5951
Fe		0.1952	0.1915	0.1850
Ni		1.9525	1.9153	1.8496
Cr		1.6780	2.9923	5.3133
Zr		1.9525	1.9153	1.8496

Compositions Weight percent:
*

Zr	Nb	Hf
98.97	1.0	0.03

Table 3-7. Control Rod Design Parameters

Parameter	Units	Value
Clad Inner Diameter	cm	0.700
Clad Thickness	cm	0.06
Clad Material		Stainless Steel*
Absorber Diameter	cm	0.700
Absorber Material		Natural B4C**
Absorber Density	g / cc	1.80

Compositions Weight percent:

*

C	Cr	Ni	Ti	Fe
0.12	18.5	10.5	1.0	69.88

**** Content of ^{10}B is 19.8% atoms.**

Remark. The lower part (30 cm) of control rods consists of Dy_2O_3 TiO2 of density 4.9 g / cc.

Fig.3-1 . Simplified Design for 3-Zones MOX assembly

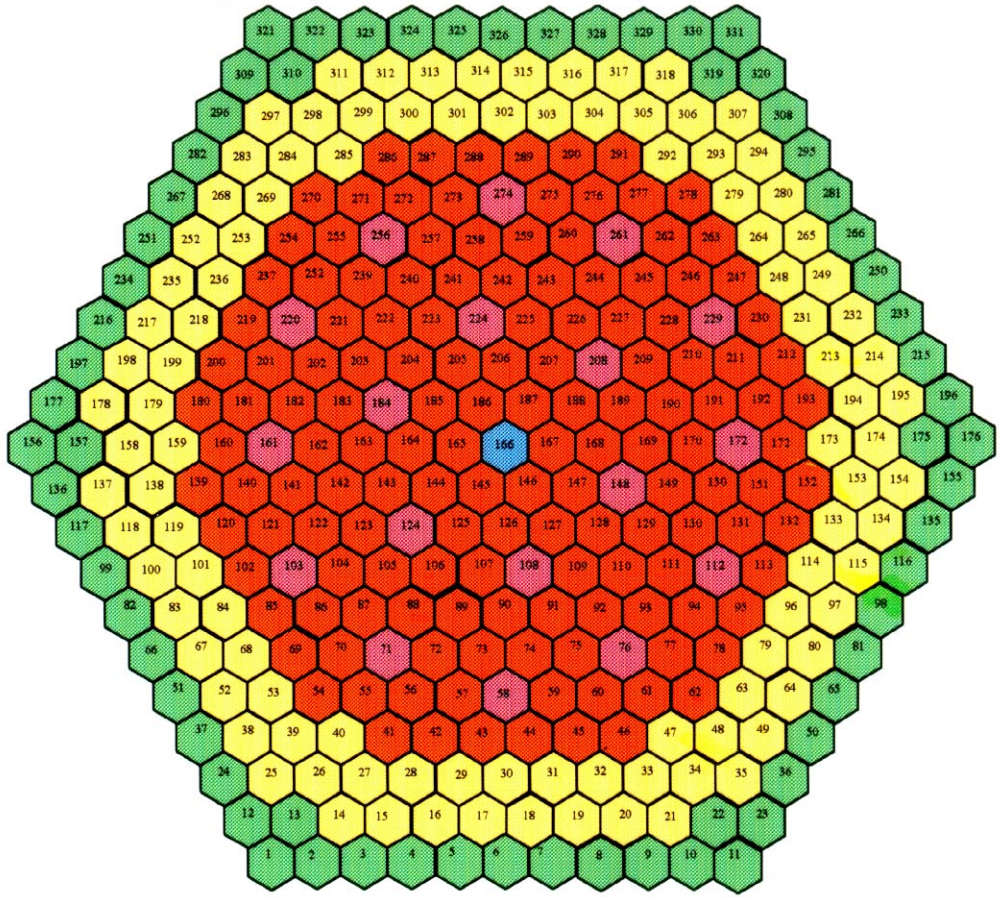

2.0% fissile Pu MOX Rods

3.0% fissile Pu MOX Rods

4.2% fissile Pu MOX Rods

Central tube

Guide Tube

Fig.3-2. Simplified Design for VVER-1000 Fuel Assembly. Type A

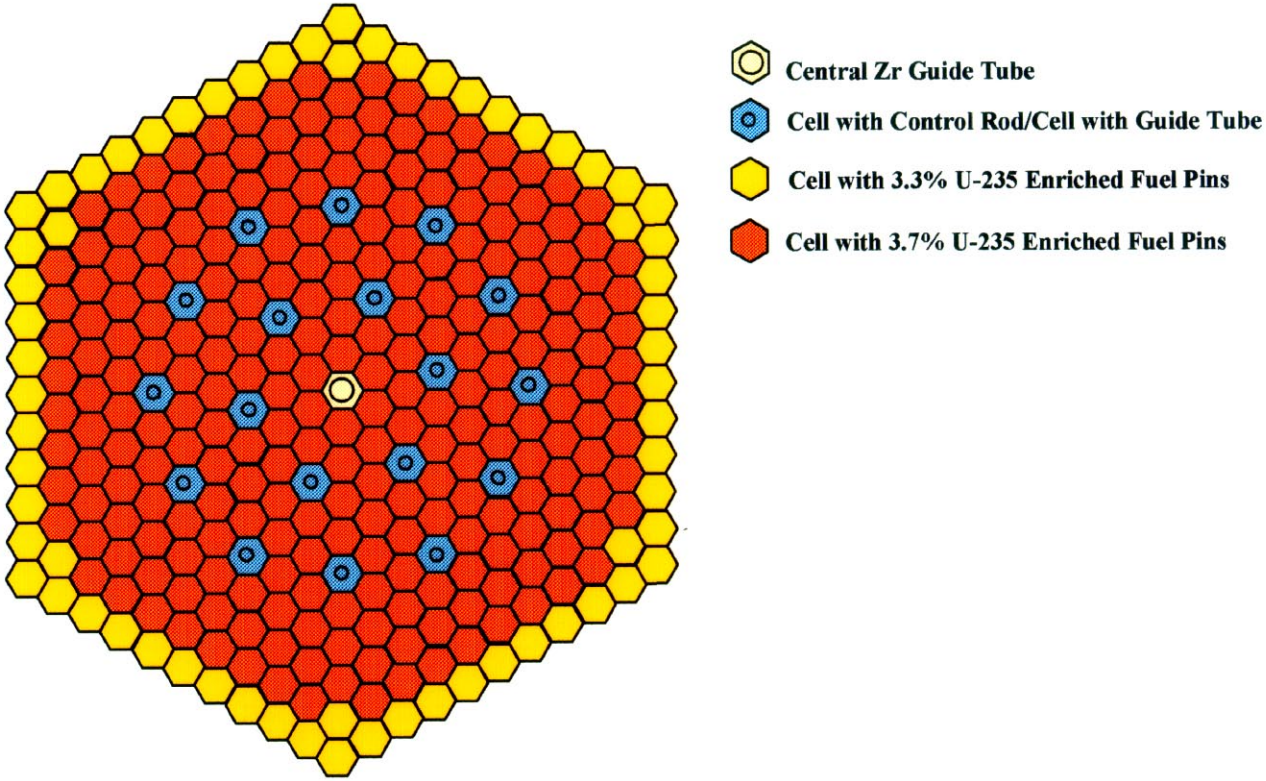

Fig.3-3. Simplified Design for VVER-1000 Fuel Assembly. Type B, Ba and Bb

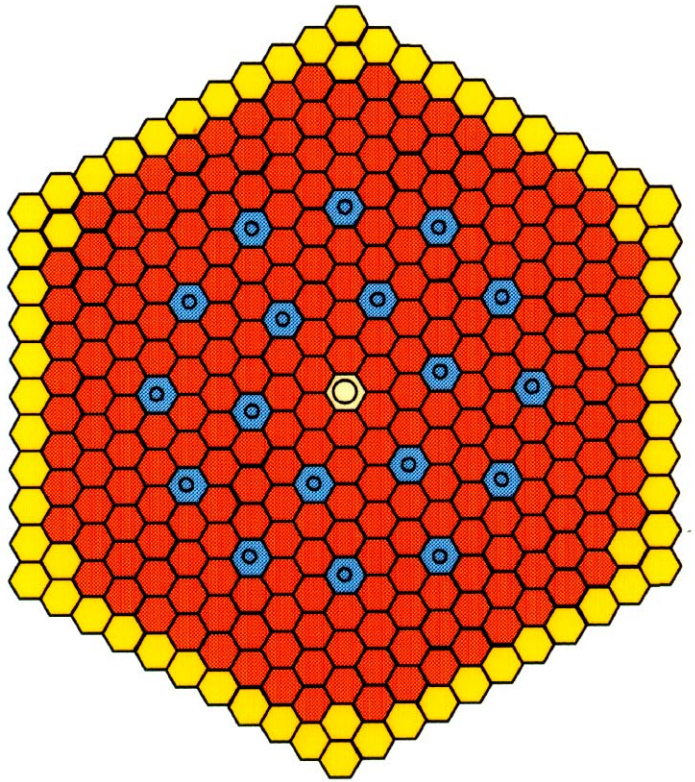

Central Zr Guide Tube

Cell with Burnable Absorber/Cell with Guide Tube

Cell with 3.3% U-235 Enriched Fuel Pins

Cell with 3.7% U-235 Enriched Fuel Pins

B - (0,065 g/cc Boron BPRs, removed after 1st year)

Ba - (0,036 g/cc Boron BPRs, removed after 1st year)

Bb - (0,020 g/cc Boron BPRs, removed after 1st year)

Fig.3-4. Simplified Design for VVER-1000 Fuel Assembly. Type C

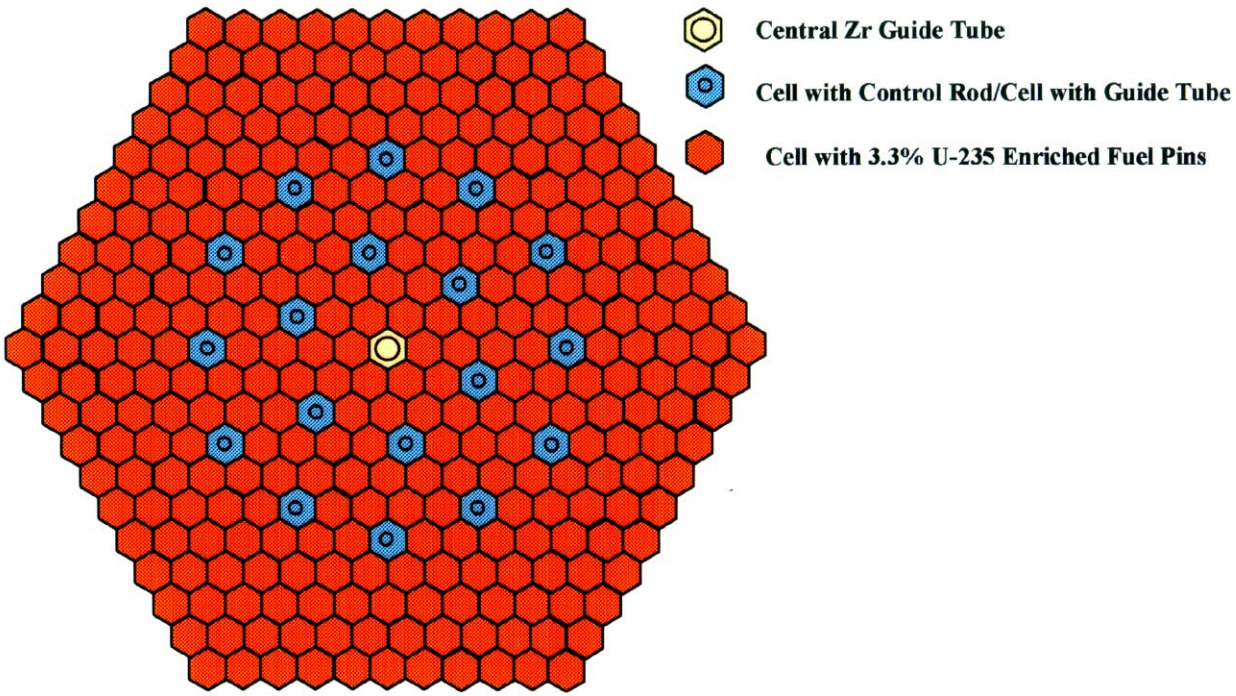

Fig.3-5. Equilibrium Loading Pattern for Base Uranium Core with Boron BPRs, Core 60° Sector

An - 3,7% Enrichment graded by 3,3% Replaced After 3 Years (No BPRs)

Bn - 3,7% Enrichment graded by 3,3% Replaced After 3/4 Years (0,065 g/cc Boron BPRs, removed after 1st year)

Cn - 3,3% Enrichment Replaced After 3 Years (No BPRs)

1-28 - Positions in 60 Degree Sector

n - Current Cycle of Fuel Assembly

Symbol e.g. **$** - Position of a Fuel Assembly During Lifetime in Core

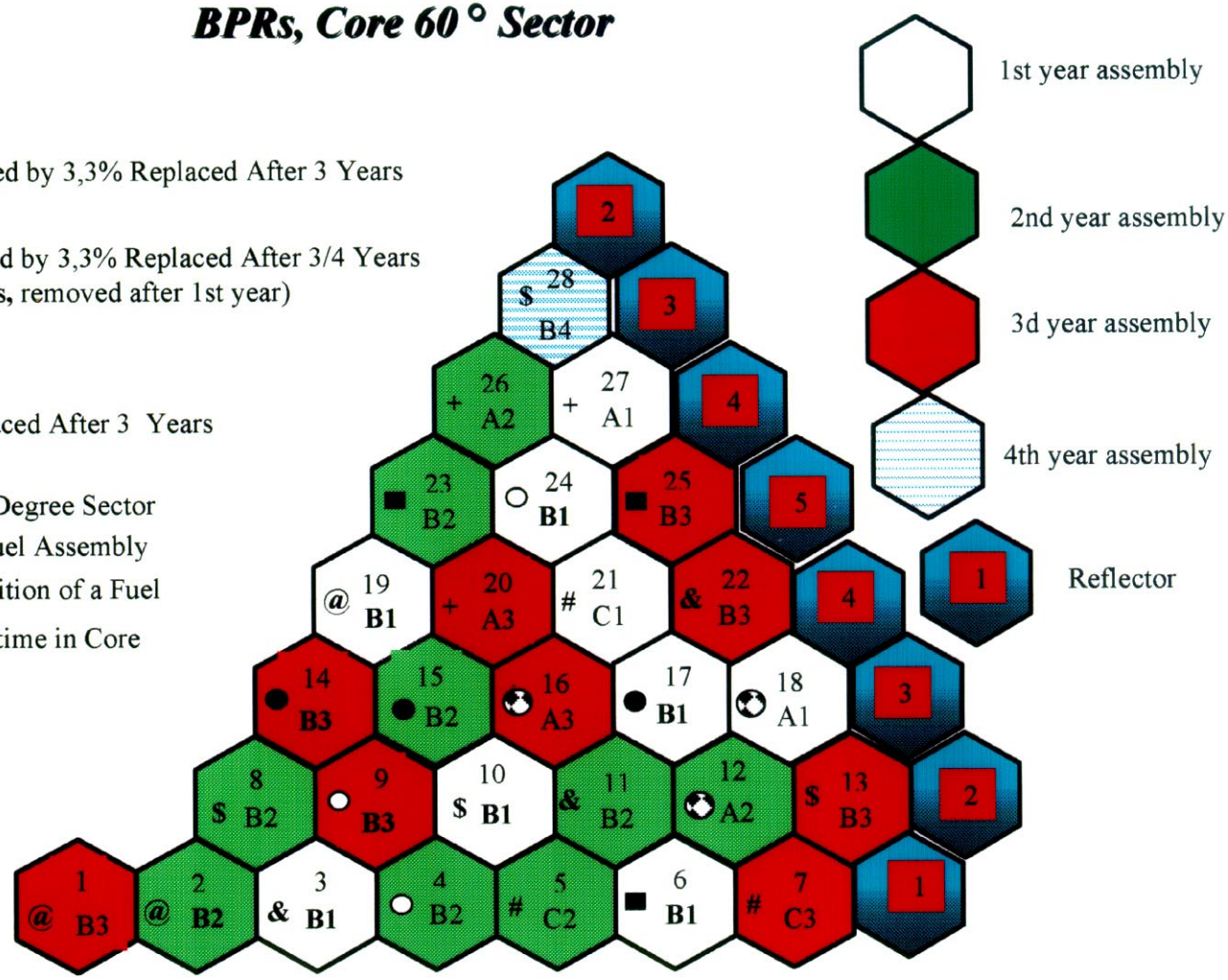

BURNUP(KG F-P/T FUEL) BOC
BURNUP(KG F-P/T FUEL) EOC
RELATIVE POWER BOC
RELATIVE POWER EOC

28						
3.4552E+01						
3.7970E+01						
2.9703E-01						
3.7042E-01						
26	27					
9.4878E+00	0.0000E+00					
2.0191E+01	7.9323E+00					
1.0155E+00	7.2646E-01					
1.0601E+00	8.0797E-01					
23	24	25				
1.4940E+01	0.0000E+00	3.0004E+01				
2.7518E+01	1.1910E+01	3.5474E+01				
1.2434E+00	1.1149E+00	4.9584E-01				
1.1993E+00	1.1848E+00	5.6691E-01				
19	20	21	22			
0.0000E+00	2.2363E+01	0.0000E+00	3.0316E+01			
1.3348E+01	3.3883E+01	1.2624E+01	3.5767E+01			
1.3011E+00	1.1420E+00	1.2370E+00	4.9398E-01			
1.2859E+00	1.0971E+00	1.2025E+00	5.6514E-01			
14	15	16	17	18		
2.9106E+01	1.4296E+01	2.2474E+01	0.0000E+00	0.0000E+00		
3.9180E+01	2.6576E+01	3.3950E+01	1.1882E+01	7.9817E+00		
1.0037E+00	1.2318E+00	1.1365E+00	1.1111E+00	7.3092E-01		
9.6843E-01	1.1608E+00	1.0941E+00	1.1831E+00	8.1290E-01		
8	9	10	11	12	13	
1.6166E+01	2.8873E+01	0.0000E+00	1.5729E+01	9.5718E+00	3.0550E+01	
2.8153E+01	3.8955E+01	1.3314E+01	2.8146E+01	2.0285E+01	3.4214E+01	
1.2283E+00	1.0024E+00	1.2964E+00	1.2247E+00	1.0154E+00	3.1949E-01	
1.1225E+00	9.7048E-01	1.2839E+00	1.1868E+00	1.0619E+00	3.9543E-01	
1	2	3	4	5	6	7
3.0565E+01	1.6180E+01	0.0000E+00	1.4294E+01	1.5026E+01	0.0000E+00	2.9914E+01
4.0498E+01	2.8270E+01	1.2886E+01	2.5894E+01	2.7341E+01	1.2419E+01	3.5531E+01
1.0298E+00	1.2611E+00	1.2748E+00	1.1859E+00	1.2374E+00	1.1684E+00	4.9960E-01
9.2825E-01	1.1160E+00	1.2372E+00	1.0874E+00	1.1626E+00	1.2325E+00	5.9583E-01

Fig. 3-6. Uranium Zone. Assembly Burnup, Relative Power

Fig.3-7. Equilibrium Loading Pattern for MOX Fueled Core with 54 MOX Fuel Assemblies, Core 60 ° Sector

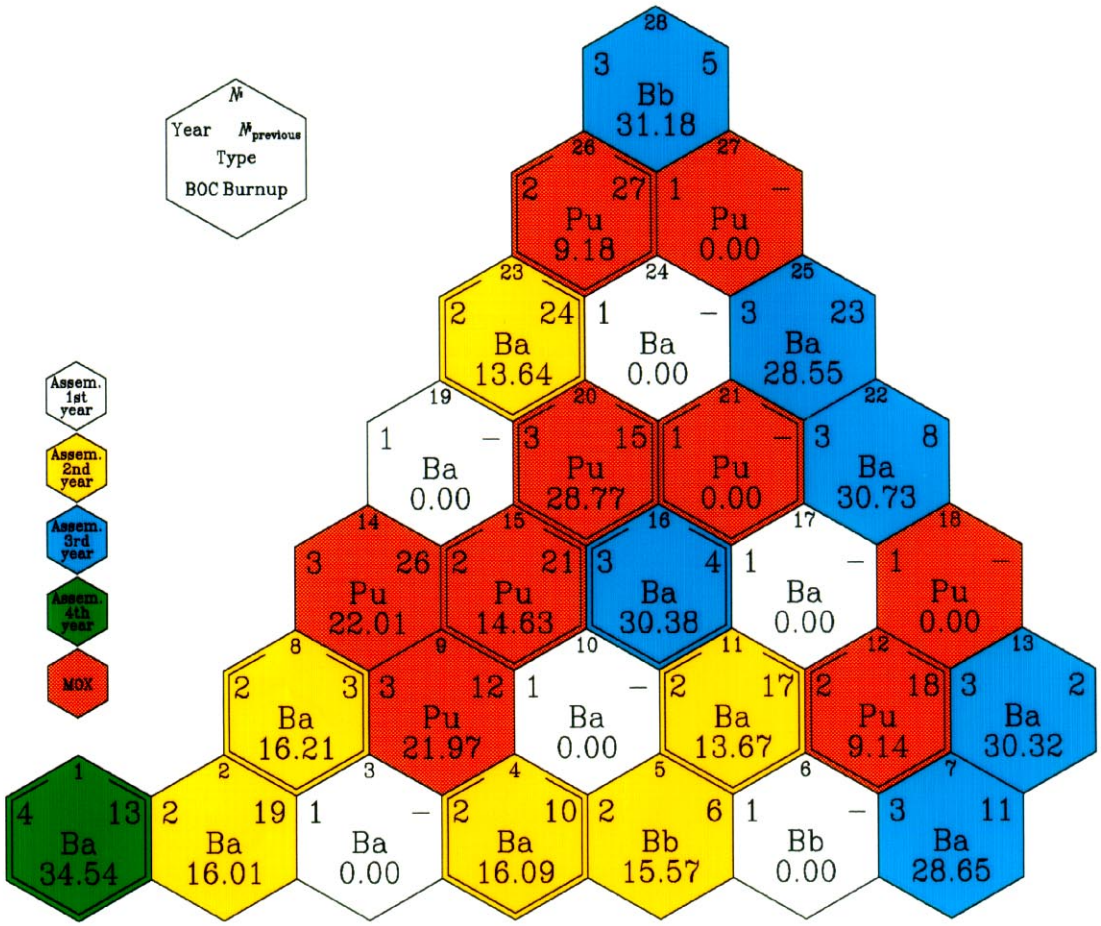

```
BURNUP(KG F-P/T FUEL) BOC
BURNUP(KG F-P/T FUEL) EOC
RELATIVE POWER  BOC
RELATIVE POWER  EOC

   28
3.1184E+01
3.4611E+01
3.0911E-01
3.6668E-01
   26          27
9.1836E+00 0.0000E+00
1.9963E+01 7.6534E+00
1.0584E+00 7.5555E-01
1.0438E+00 7.5180E-01
   23          24          25
1.3641E+01 0.0000E+00 2.8555E+01
2.6270E+01 1.1354E+01 3.3750E+01
1.2428E+00 1.0802E+00 4.8501E-01
1.2081E+00 1.1276E+00 5.4117E-01
   19          20          21          22
0.0000E+00 2.8772E+01 0.0000E+00 3.0726E+01
1.3391E+01 3.8934E+01 1.2318E+01 3.5754E+01
1.2865E+00 9.8680E-01 1.2676E+00 4.6736E-01
1.2901E+00 9.9787E-01 1.1672E+00 5.2600E-01
   14          15          16          17          18
2.2005E+01 1.4628E+01 3.0380E+01 0.0000E+00 0.0000E+00
3.3415E+01 2.6481E+01 3.9966E+01 1.1393E+01 7.6270E+00
1.1244E+00 1.1721E+00 9.1902E-01 1.0780E+00 7.5038E-01
1.0915E+00 1.1323E+00 9.5212E-01 1.1362E+00 7.5113E-01
    8           9          10          11          12          13
1.6211E+01 2.1966E+01 0.0000E+00 1.3671E+01 9.1446E+00 3.0319E+01
2.8526E+01 3.3381E+01 1.3474E+01 2.6372E+01 1.9925E+01 3.3796E+01
1.2107E+00 1.1246E+00 1.2905E+00 1.2451E+00 1.0560E+00 3.1349E-01
1.1759E+00 1.0923E+00 1.3013E+00 1.2189E+00 1.0458E+00 3.7203E-01
    1           2           3           4           5           6           7
3.4539E+01 1.6012E+01 0.0000E+00 1.6089E+01 1.5566E+01 0.0000E+00 2.8649E+01
4.3881E+01 2.8247E+01 1.3614E+01 2.7752E+01 2.8780E+01 1.3136E+01 3.4671E+01
8.9037E-01 1.1985E+00 1.3071E+00 1.1637E+00 1.3092E+00 1.2636E+00 5.5245E-01
9.2900E-01 1.1750E+00 1.3088E+00 1.1019E+00 1.2500E+00 1.2618E+00 6.2459E-01
```

Fig. 3-8. MOX Zone. Assembly Burnup, Relative Power.

Fig.3-9. Control Rods Grouping and Positions of in-core self-powered detectors

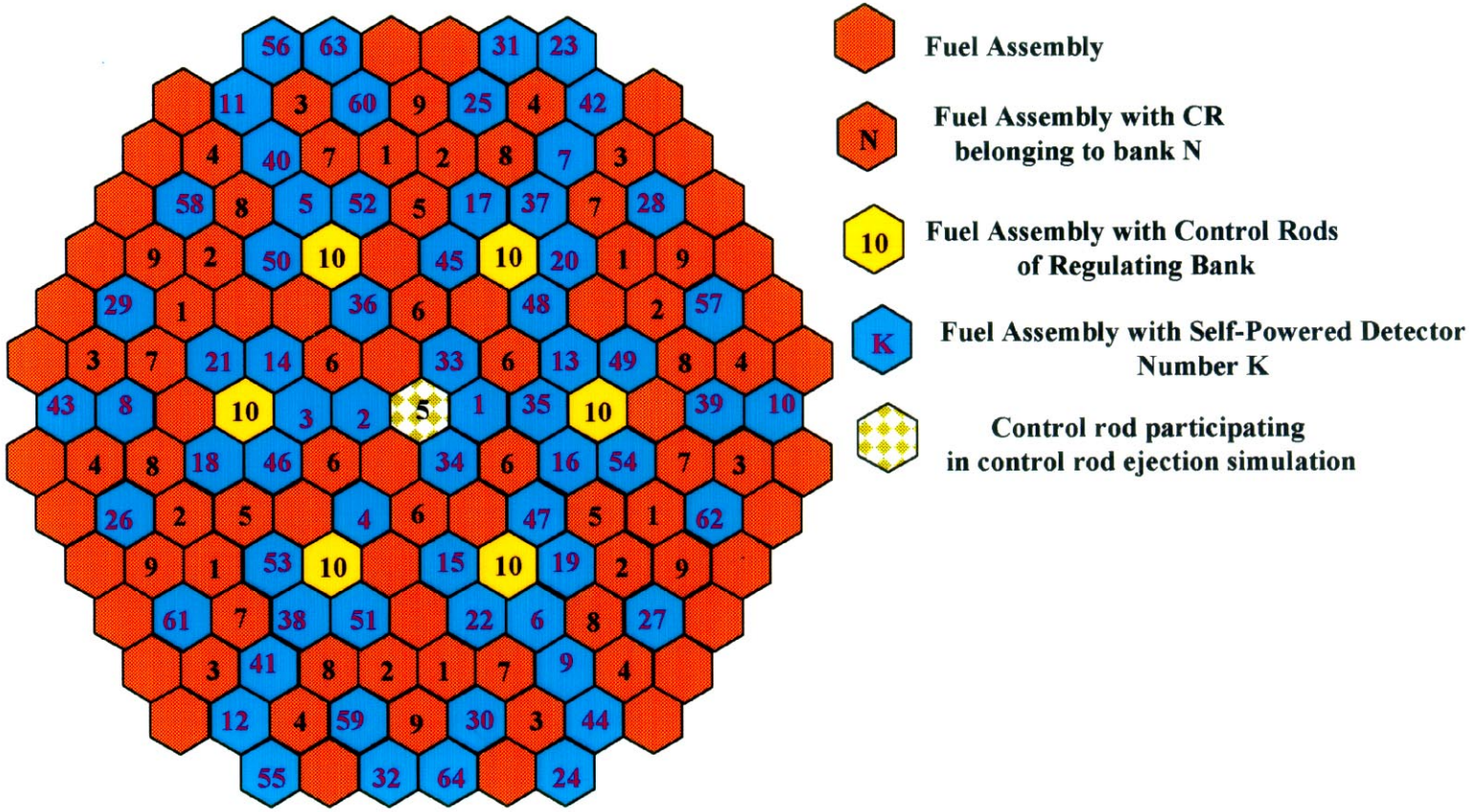

Fig.3-10. Assemblies Numeration in VVER-1000 Core

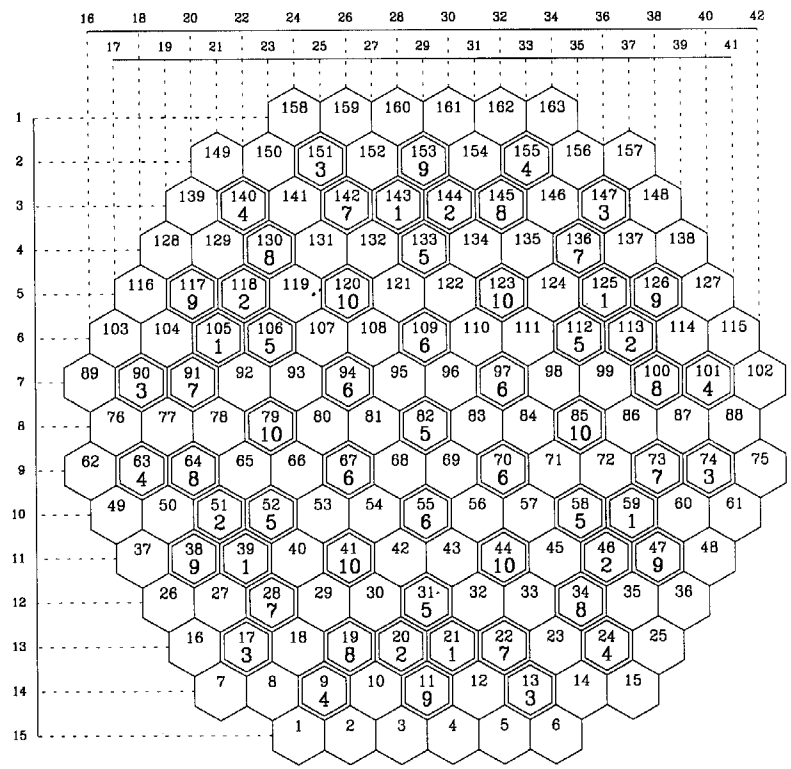

– Number of Fuel Assembly

– Number of Banks

Fig.3-11. Model of VVER-1000 Reflector

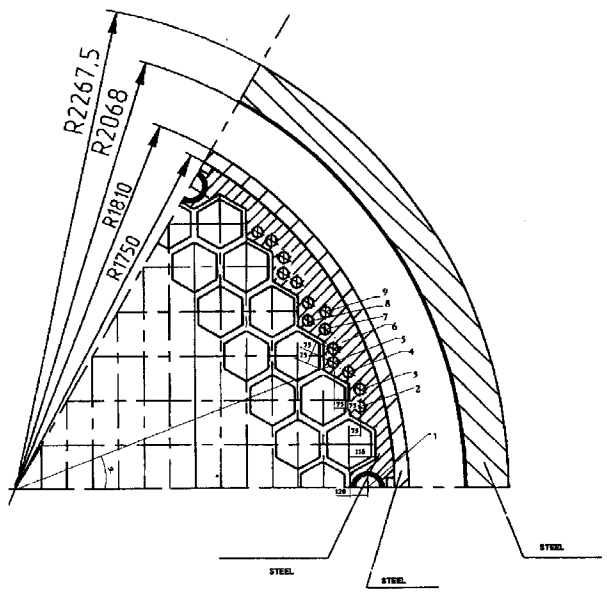

Hole number	Distance from core center (R)	Angle (φ°)	Hole diameter
	mm		mm
1	1655	0	98
2	1655	13	70
3	1675	16	70
4	1655	19	70
5	1600	21	70
6	1635	24	70
7	1625	27	70
8	1575	30	70
9	1665	30	70

Fig. 3-12. Reflector "Assembly" of Type 1

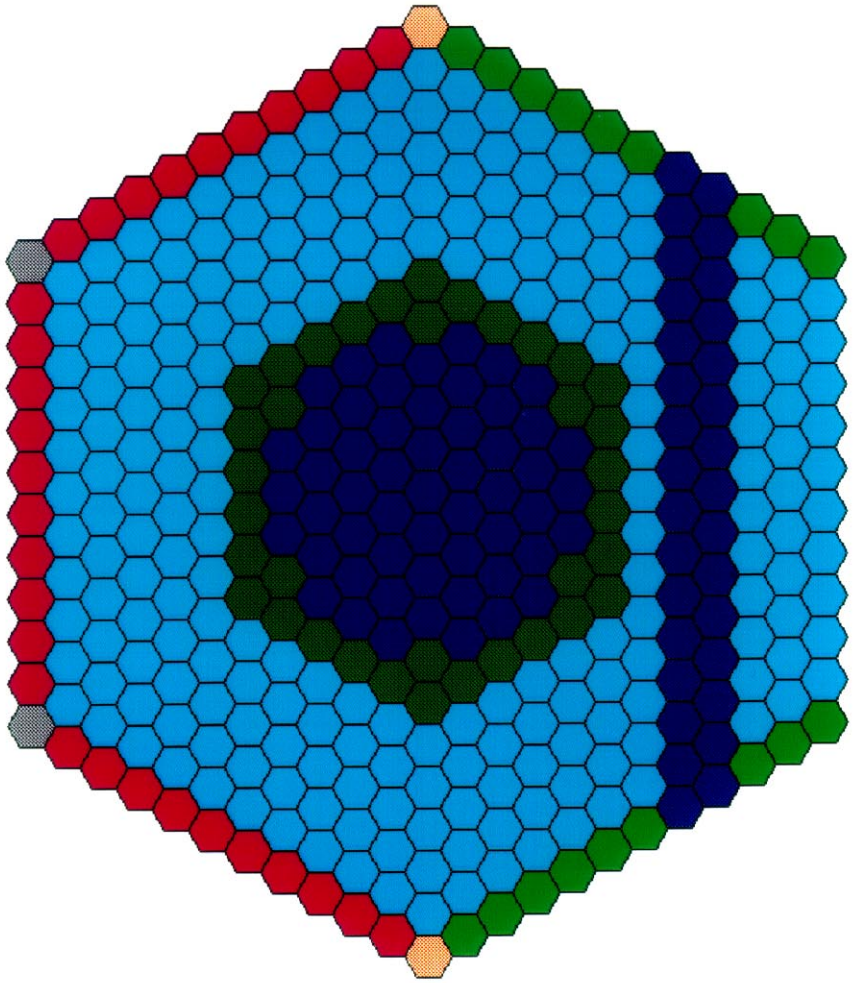

Steel 100 Water 0

Steel 0 Water 100

Steel 11 Water 89

Steel 26 Water 74

Steel 50 Water 50

Steel 50 Water 50

Steel 100 Water 0

Fig. 3-13. Reflector "Assembly" of Type 2

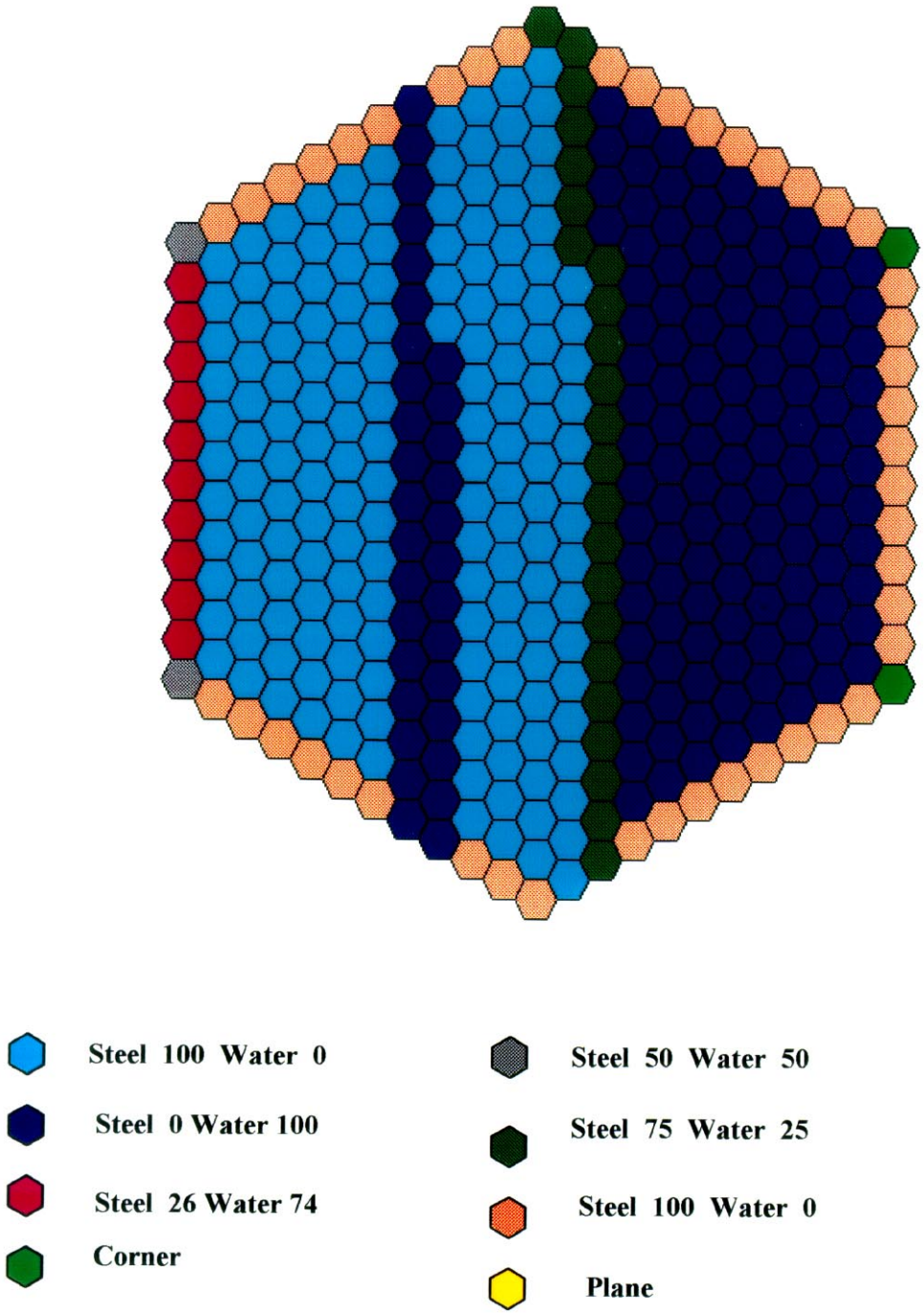

Fig. 3-14. Reflector "Assembly" of Type 3

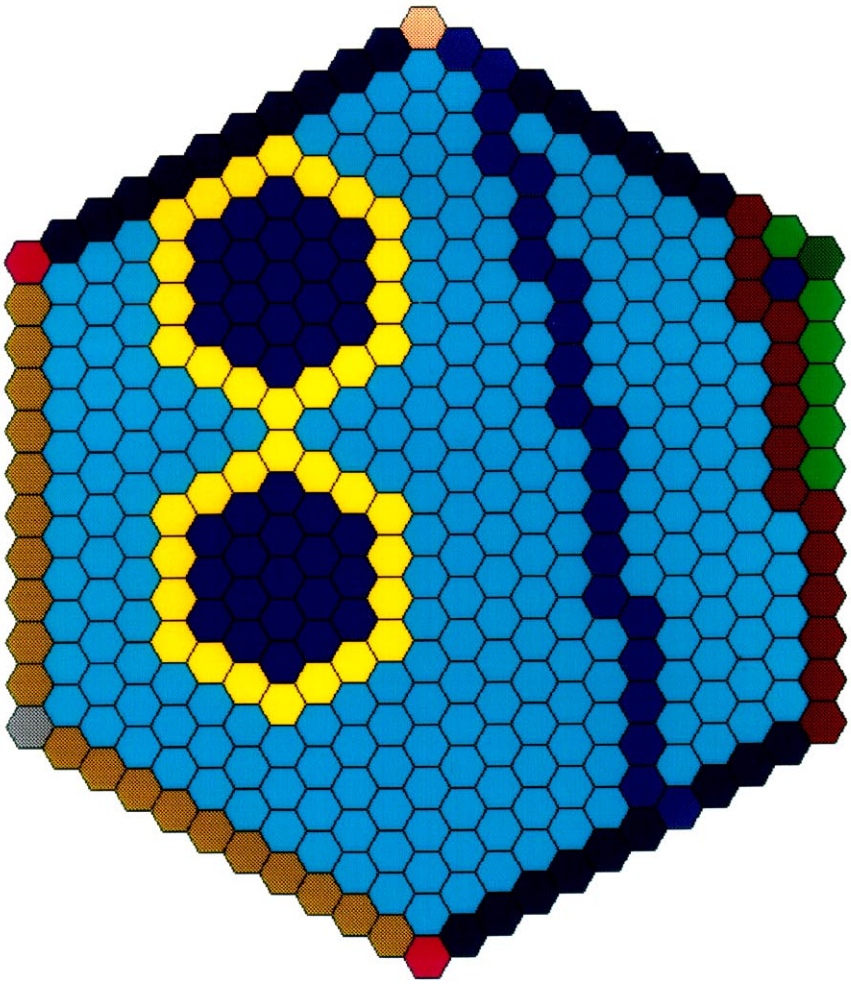

Steel 100 Water 0

Steel 0 Water 100

Steel 50 Water 50

Plane

Steel 75 Water 25

Steel 100 Water 0

Steel 11 Water 89

Corner

Steel 100 Water 0

Steel 50 Water 50

Steel 26 Water 74

Fig. 3-15. Reflector "Assembly" of Type 4

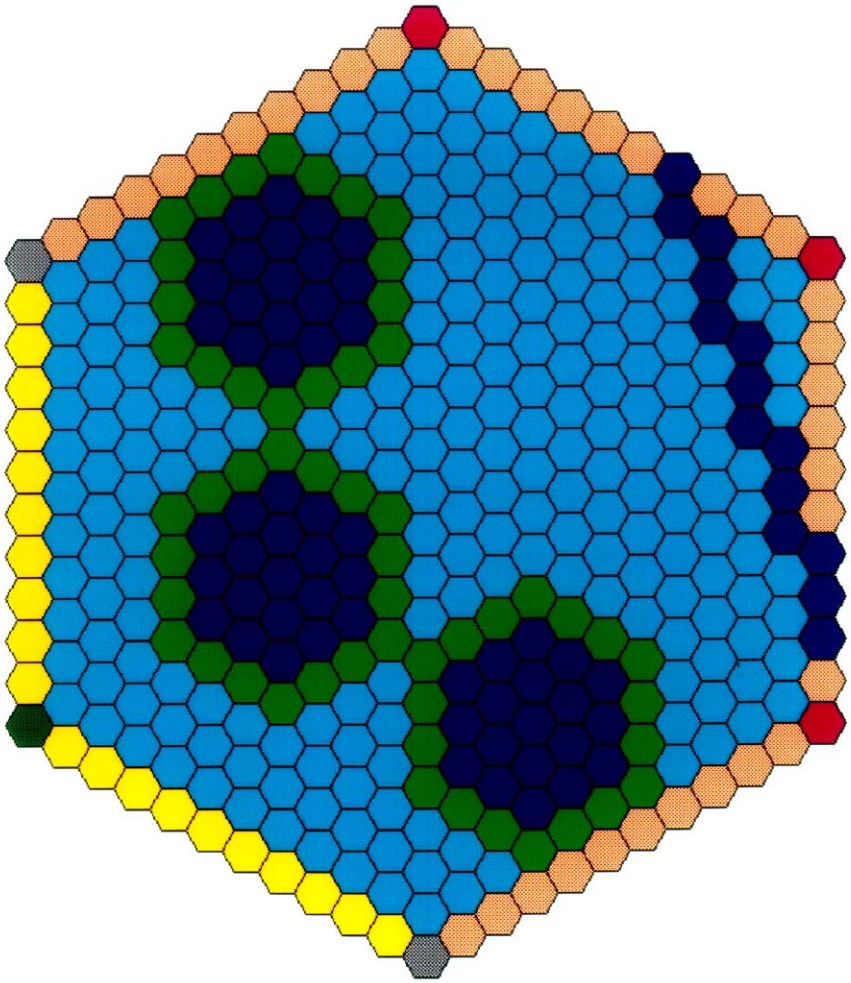

Steel 100 Water 0

Steel 0 Water 100

Steel 100

Steel 50 Water 50

Steel 50 Water 50

Steel 11 Water 89

Steel 100 Water 0

Steel 26 Water 74

Fig. 3-16. Reflector "Assembly" of Type 5

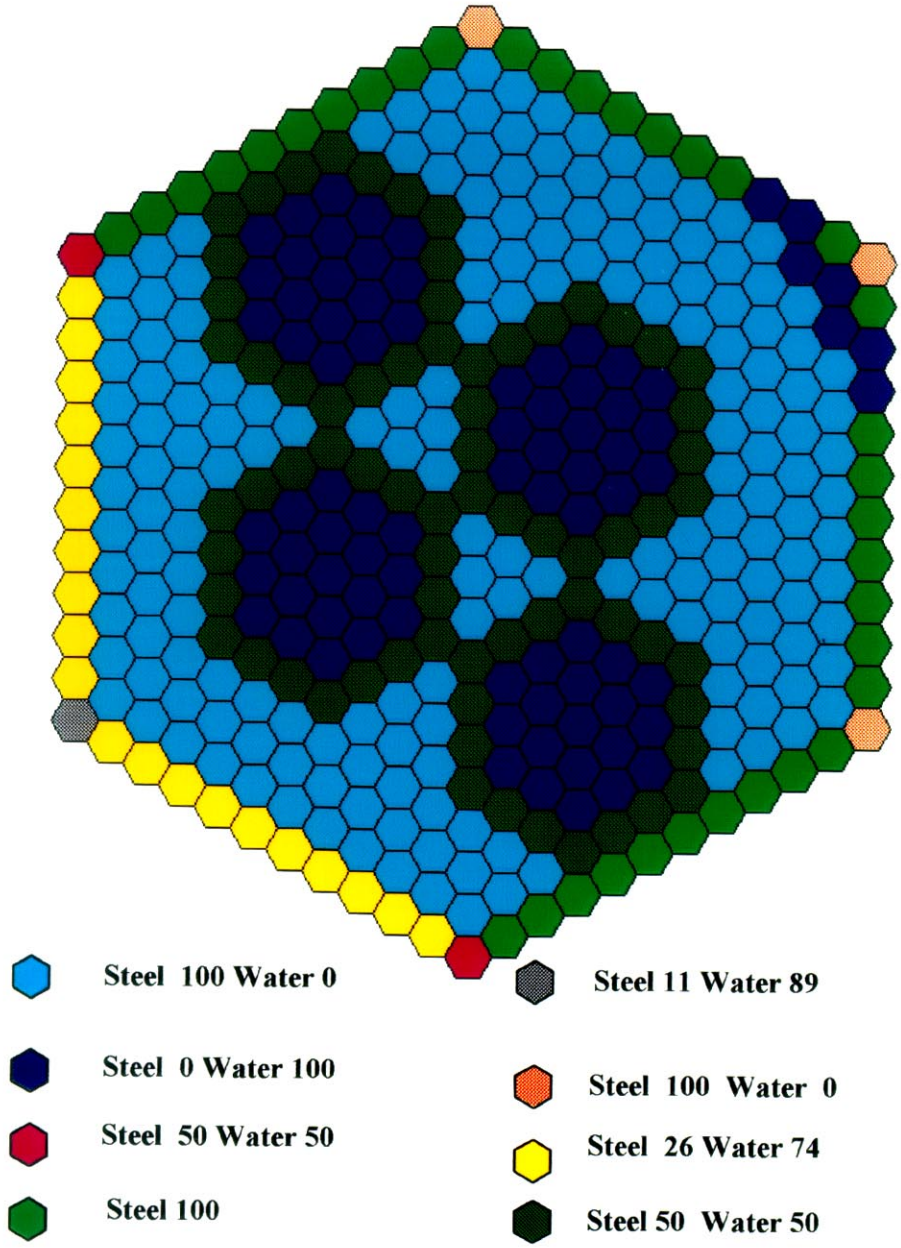

Fig.3-17. Core Design. Material Contents (Vol%) in Axial Direction

Zone	HzO	St.-Steel	Zr	He
A	58.0	0	42.0	0
B	57.0	33.0	10.0	0
C	67.0	33.0	0	0
D	56.0	0	13.8	30.2
E	56.0	0	32.5	11.5
F	98.9	0	0	0

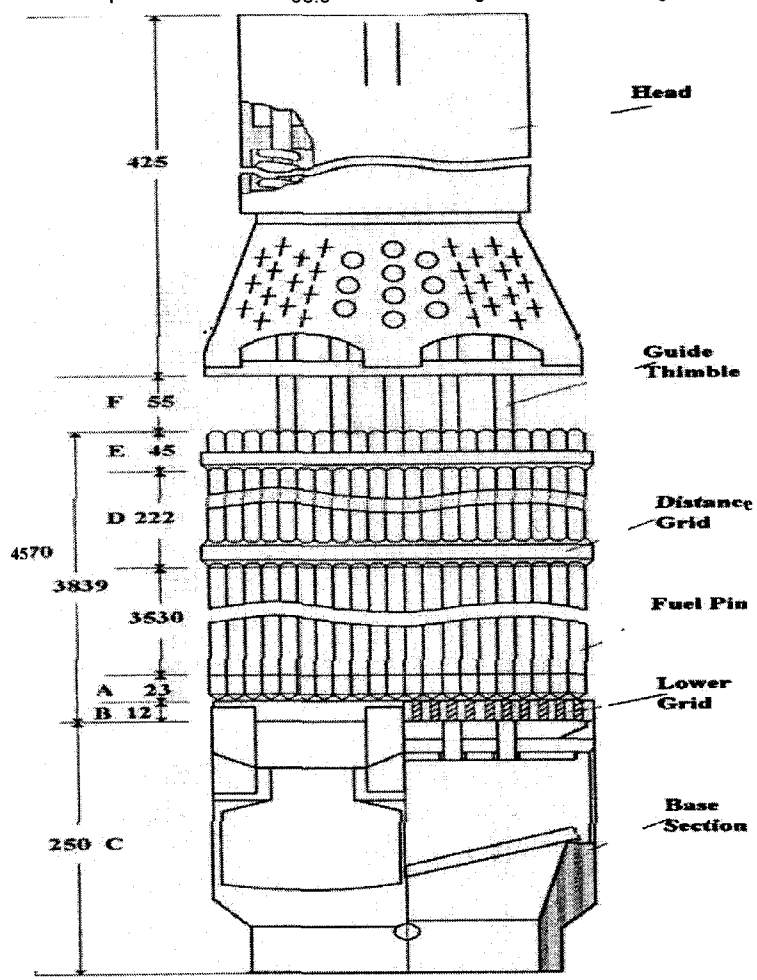

4. Central Control Rod Ejection from the VVER-1000 Core

4.1. *Process being investigated*: Central control rod is ejected by pressure drop caused by destroying of the moving mechanism cover.

4.2. *Initial state of the core*:

- EOC for equilibrium refueling regime, see Figures 4-1, 4-2.
- Thermal power of reactor - nominal power level W_{nom}.
- Coolant flow rate - 84 000 m^3/h.
- Positions of control rods regulating bank and central control rod are - 20% from the core bottom.
- Xenon and samarium concentrations - equilibrium values corresponding to the reactor nominal power level.

4.3. *Scenario of transient.*

Central control rod is ejected by pressure drop caused by destroying of the moving mechanism cover. Time point of ejection start corresponds to 0.1 sec. Initial control rod position - 20% from the core bottom. Duration of ejection is 0.05 sec. The scram is actuated at time point 1.0 sec. Duration of the rod drop is 4 sec.

4.4. *Main calculation results.*

For the uranium zone the worth of ejected cluster is 87.4 pcm, and for the MOX zone it is 93.6 pcm.

The calculation results of dynamical processes are shown in Figs. 4-3 - 4-8. Figs. 4-5 - 4-8 present the characteristics of «hot» channel with sampling all over the core.

The «hot» channel power was taken as

$q_{hot.chan.ij}=q_{ij}*K_{eng}*K_k^{max}$,

where q_{ij} is the power averaged over the calculation prism ij, with j being the number of layer in the core height; i - the FA number;

K_{eng} - is the engineering margin coefficient accounting for the errors in the calculation of power averaged over FA cross section, q_{ij}, and of the flow rate through the i-th FA;

K_k^{max} - is the maximum radial peaking coefficient in the hottest FA.

In the present work:

$K_{eng} = 1.16$,

$K_k = 1.08$

Concluding it can be said that the transition to MOX fuel does not noticeably alter the dynamical process.

FA NUMBER
BURNUP(KG F-P/T FUEL)
RELATIVE POWER
TEMPERATURE DROP

28
3.7622E+01
4.0063E-01
1.2944E+01

26	27
1.9201E+01	7.1680E+00
1.1399E+00	8.7605E-01
3.6828E+01	2.8304E+01

23	24	25
2.6445E+01	1.0807E+01	3.4939E+01
1.2528E+00	1.2681E+00	6.1422E-01
4.0476E+01	4.0970E+01	1.9845E+01

19	20	21	22
1.2328E+01	3.2896E+01	1.1496E+01	3.5234E+01
1.2386E+00	1.1472E+00	1.2955E+00	6.1234E-01
4.0019E+01	3.7063E+01	4.1857E+01	1.9784E+01

14	15	16	17	18
3.8448E+01	2.5599E+01	3.2967E+01	1.0780E+01	7.2127E+00
8.8331E-01	1.1508E+00	1.1438E+00	1.2664E+00	8.8160E-01
2.8539E+01	3.7181E+01	3.6954E+01	4.0914E+01	2.8483E+01

8	9	10	11	12	13
2.7236E+01	3.8225E+01	1.2296E+01	2.7084E+01	1.9293E+01	3.3842E+01
1.0107E+00	8.8599E-01	1.2362E+00	1.2394E+00	1.1420E+00	4.2781E-01
3.2653E+01	2.8625E+01	3.9939E+01	4.0044E+01	3.6898E+01	1.3822E+01

1	2	3	4	5	6	7
3.9690E+01	2.7321E+01	1.1944E+01	2.5385E+01	2.6401E+01	1.1301E+01	3.4976E+01
5.8580E-01	9.5214E-01	1.0889E+00	8.3411E-01	1.1438E+00	1.2963E+00	6.4059E-01
1.8926E+01	3.0762E+01	3.5181E+01	2.6949E+01	3.6953E+01	4.1880E+01	2.0696E+01

Fig. 4-1. Uranium zone. Assembly burnup, relative power and temperature drop for control rod ejection calculation.

FA NUMBER
BURNUP(KG F-P/T FUEL)
RELATIVE POWER
TEMPERATURE DROP

28
3.4268E+01
3.9600E-01
1.2794E+01

26	27
1.8990E+01	6.9459E+00
1.1223E+00	8.1328E-01
3.6260E+01	2.6276E+01

23	24	25
2.5186E+01	1.0306E+01	3.3242E+01
1.2638E+00	1.2065E+00	5.8453E-01
4.0833E+01	3.8981E+01	1.8885E+01

19	20	21	22
1.2362E+01	3.8044E+01	1.1232E+01	3.5261E+01
1.2459E+00	1.0365E+00	1.2521E+00	5.6817E-01
4.0254E+01	3.3488E+01	4.0454E+01	1.8357E+01

14	15	16	17	18
3.2580E+01	2.5533E+01	3.9117E+01	1.0336E+01	6.9199E+00
1.0020E+00	1.1177E+00	9.9172E-01	1.2165E+00	8.1284E-01
3.2373E+01	3.6110E+01	3.2041E+01	3.9302E+01	2.6262E+01

8	9	10	11	12	13
2.7549E+01	3.2546E+01	1.2436E+01	2.5278E+01	1.8951E+01	3.3448E+01
1.0752E+00	1.0027E+00	1.2582E+00	1.2760E+00	1.1249E+00	4.0190E-01
3.4737E+01	3.2394E+01	4.0649E+01	4.1227E+01	3.6343E+01	1.2985E+01

1	2	3	4	5	6	7
4.3063E+01	2.7234E+01	1.2595E+01	2.7219E+01	2.7758E+01	1.1983E+01	3.4088E+01
5.9729E-01	1.0229E+00	1.1730E+00	8.5417E-01	1.2380E+00	1.3372E+00	6.7321E-01
1.9298E+01	3.3049E+01	3.7898E+01	2.7597E+01	3.9997E+01	4.3203E+01	2.1751E+01

Fig. 4-2. MOX zone. Assembly burnup, relative power and temperature drop for control rod ejection calculation

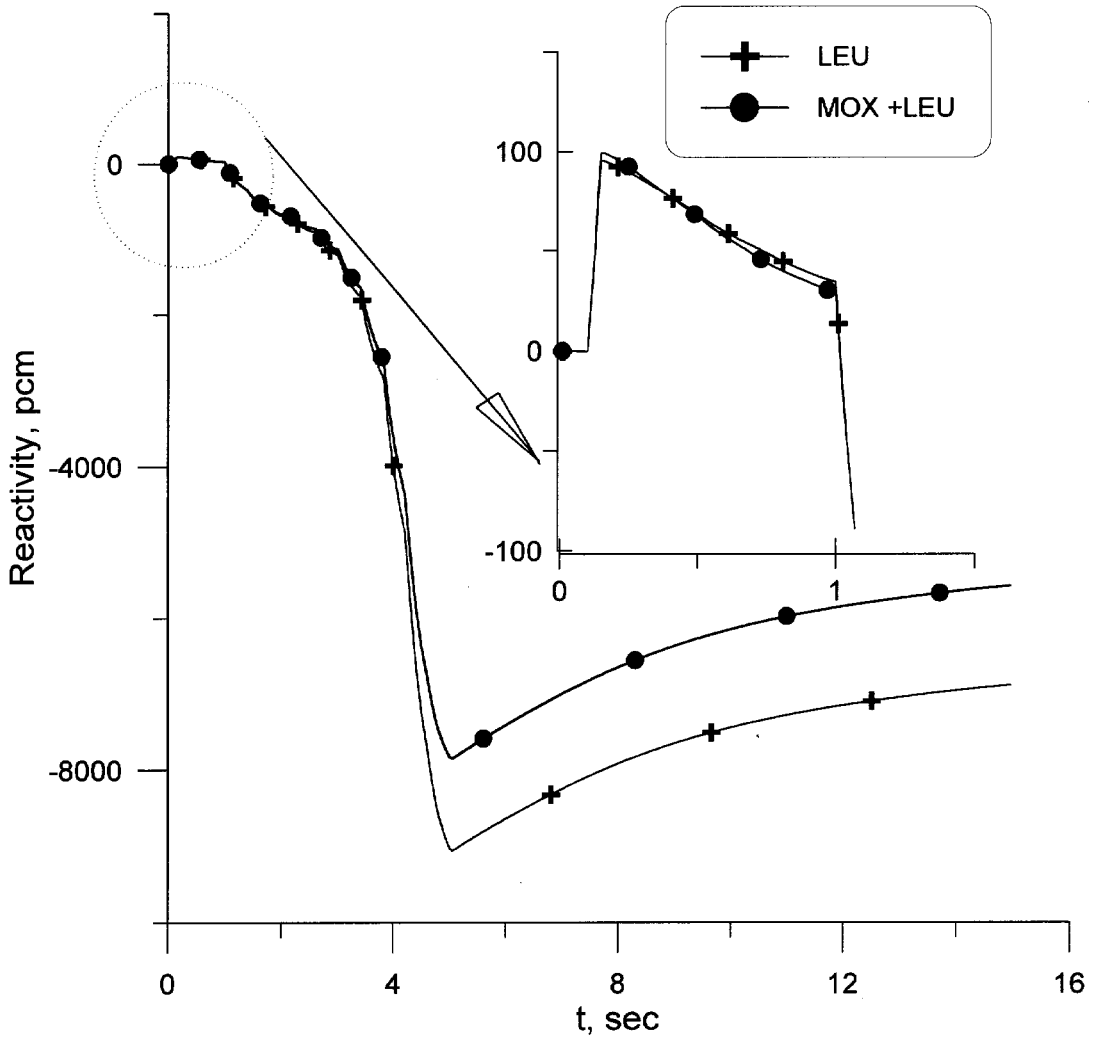

Fig. 4-3. Reactivity. Central Control Rod Ejection

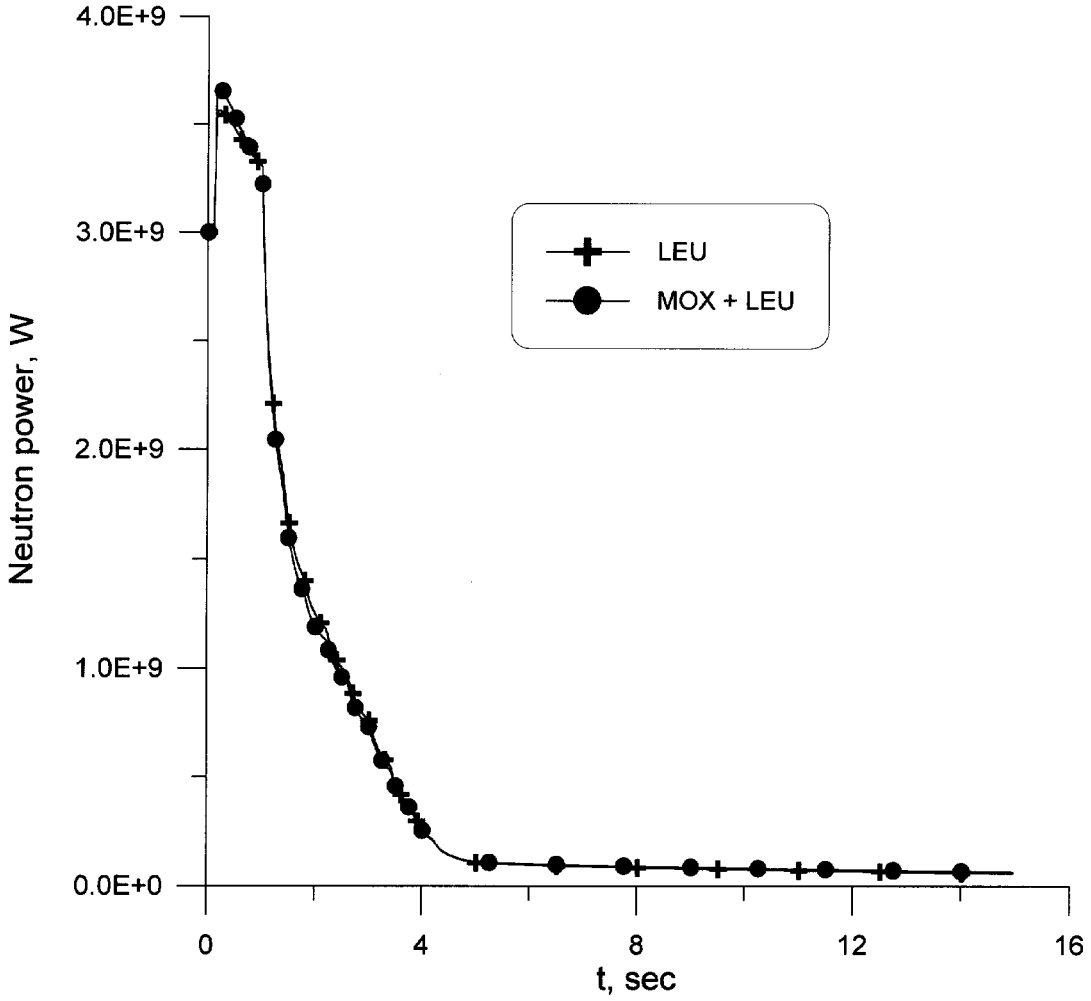

Fig. 4-4. Neutron Power. Central Control Rod Ejection

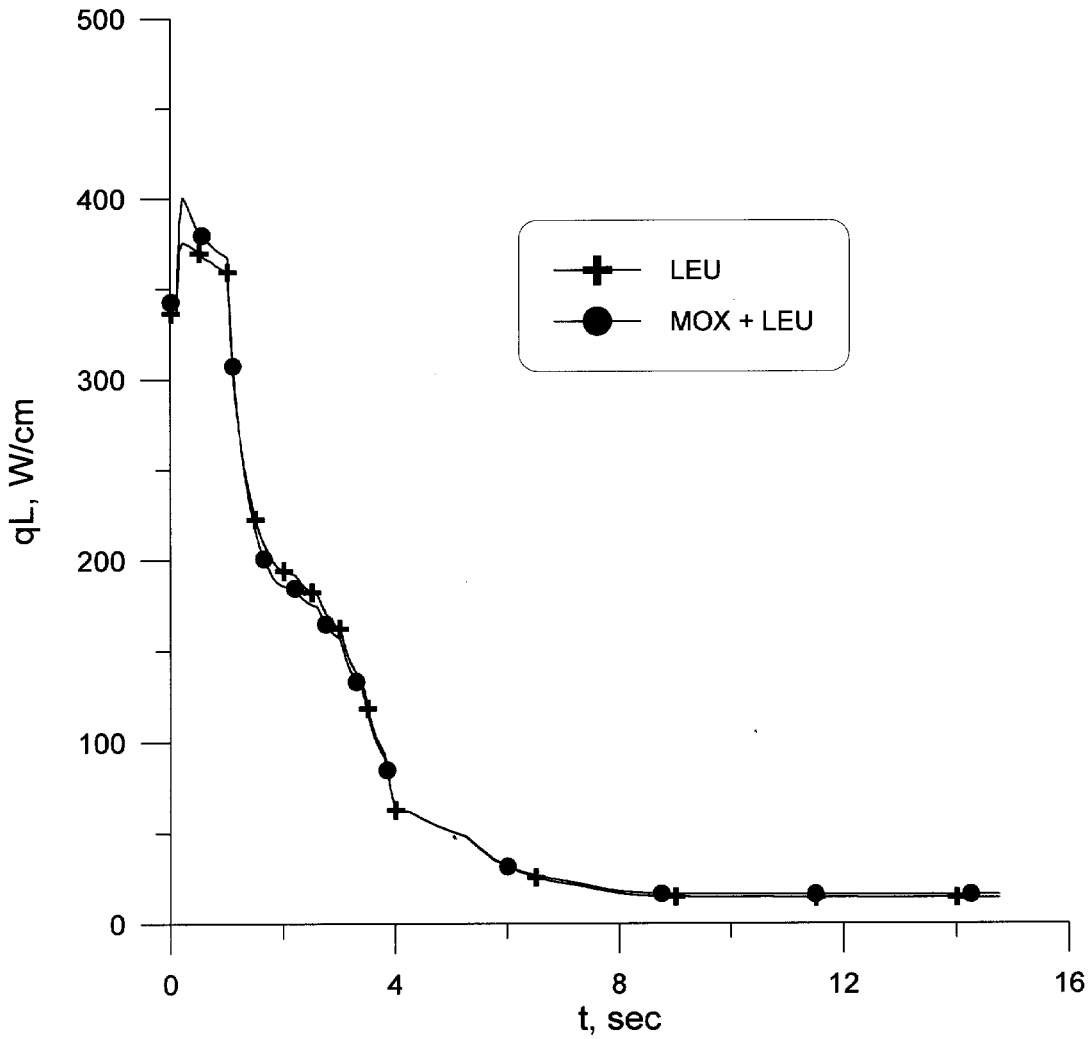

Fig. 4-5. Maximal Neutron Linear Power. Central Control Rod Ejection

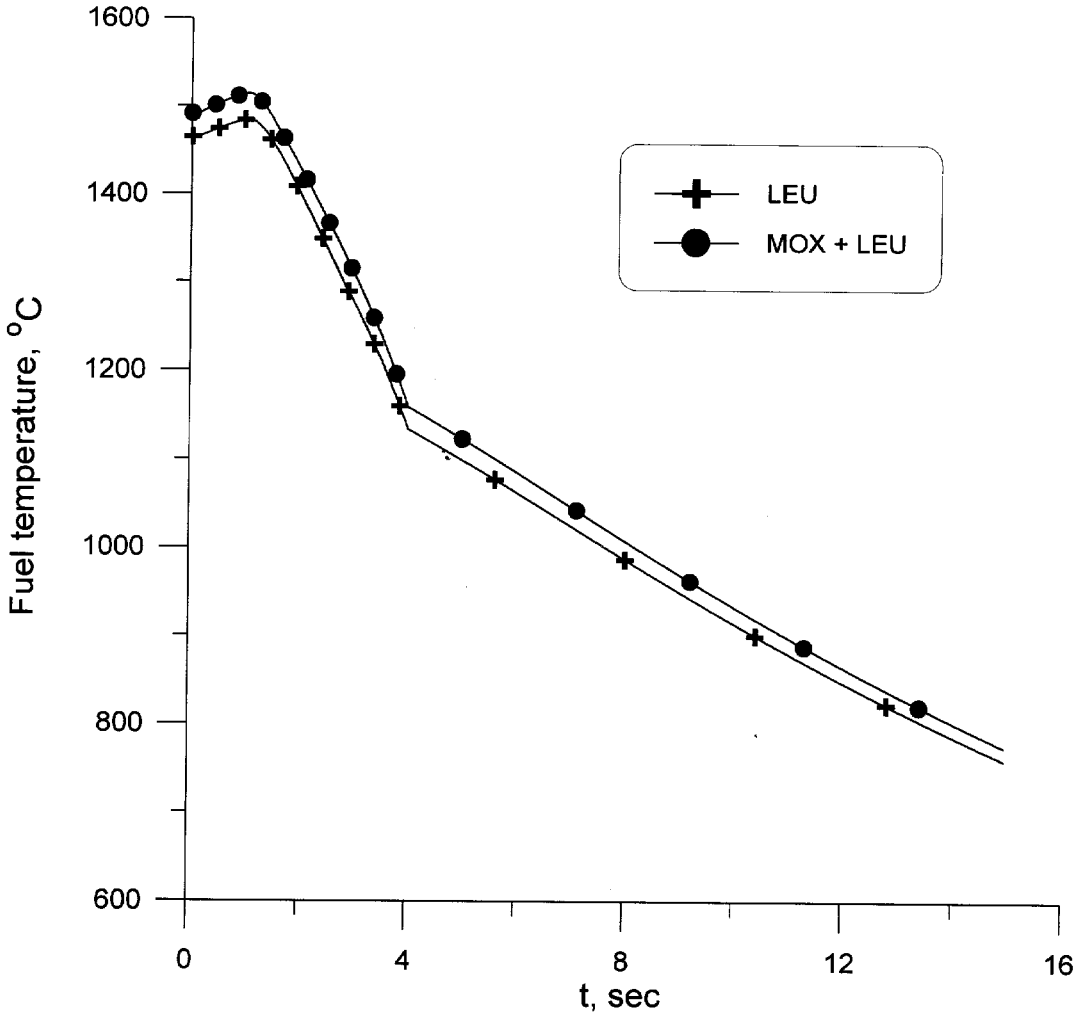

Fig. 4-6. Maximal Fuel Temperature. Central Control Rod Ejection

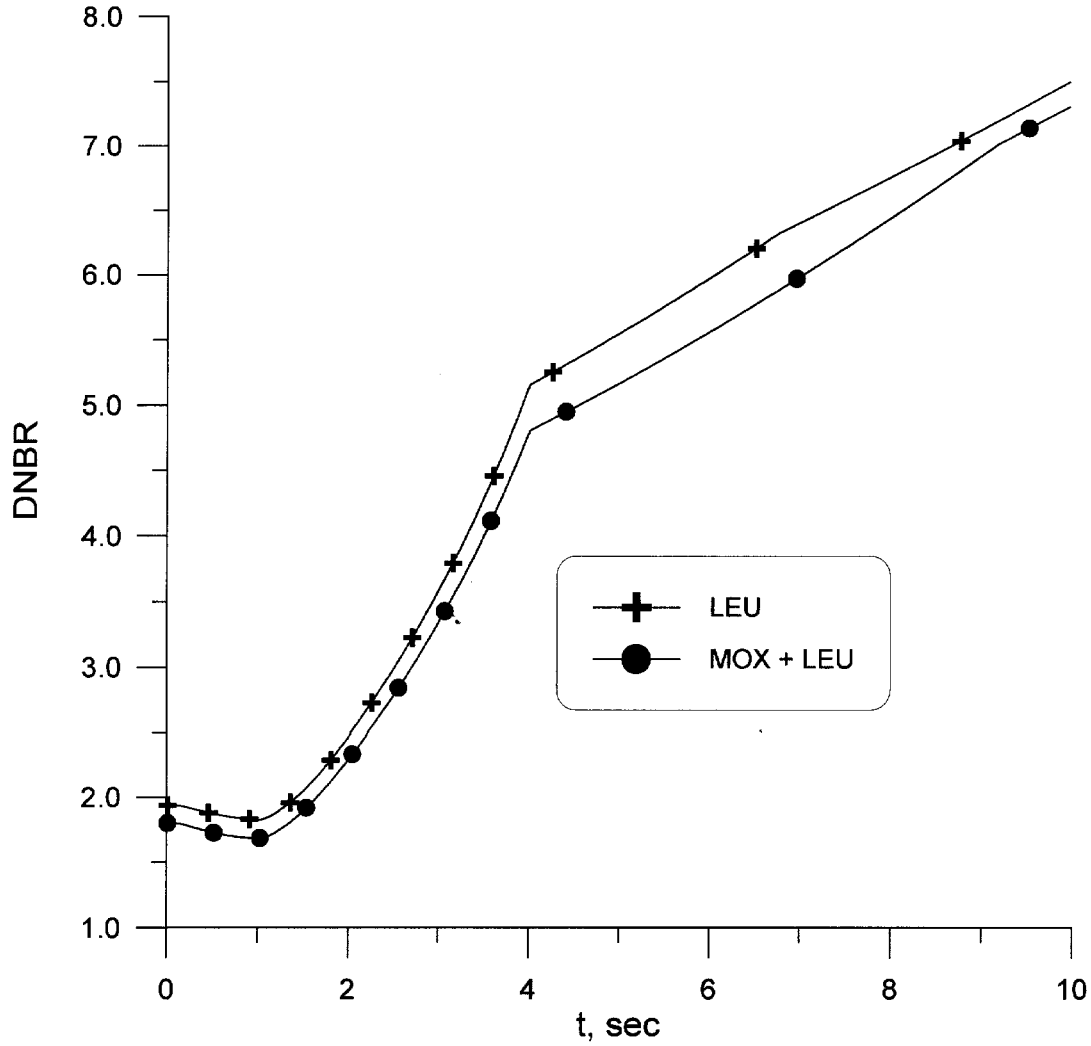

Fig. 4-7. Minimal DNBR. Central Control Rod Ejection

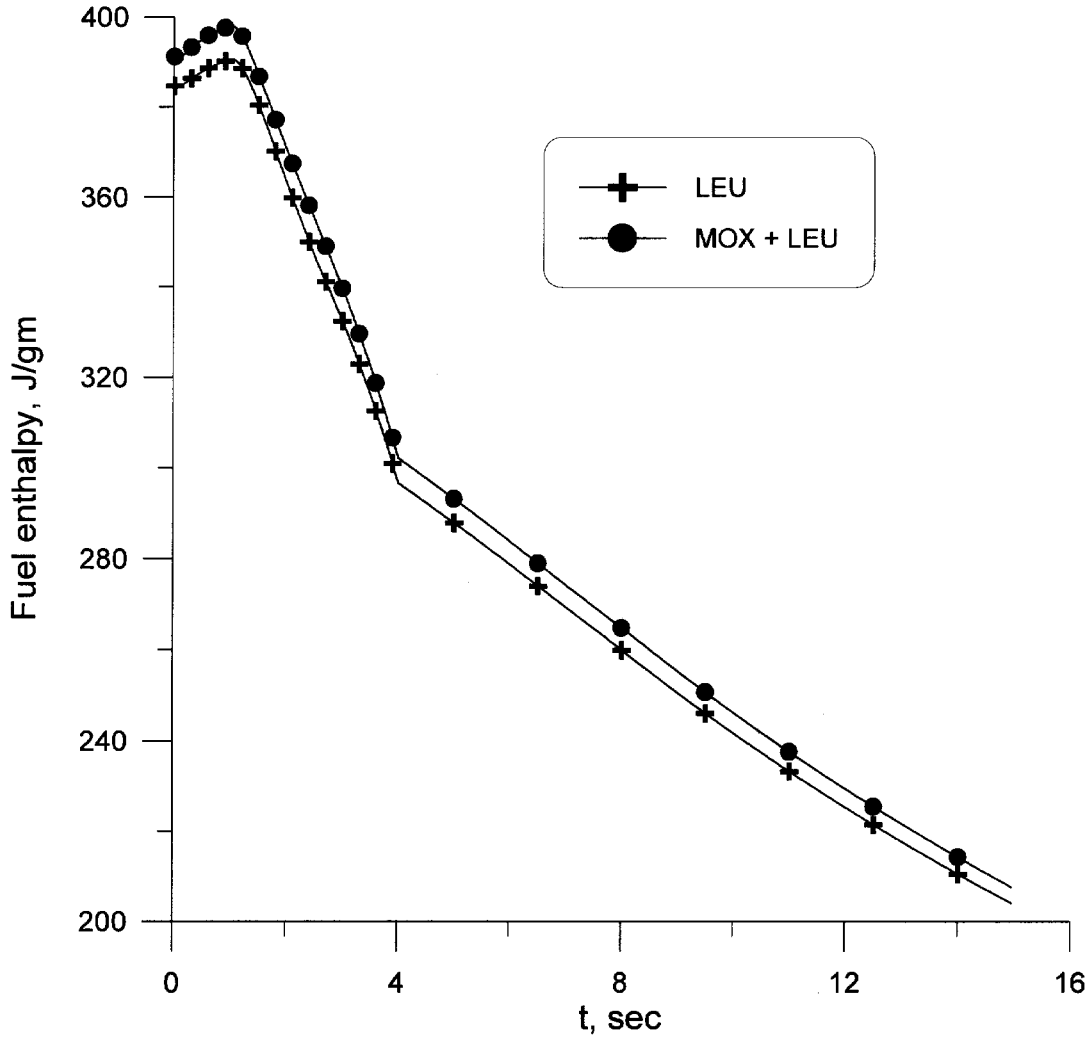

Fig. 4-8. Maximal Fuel Enthalpy. Central Control Rod Ejection

5. Core Cooling in Case of Steam Line Rupture

5.1. *Process being investigated*: Overcooling of the reactor core caused by steam line rupture and non-closure of steam generator stop valve.

5.2. *Initial state of the core*:

- EOC for equilibrium refueling regime.
- W=Wnom.
- Inlet pressure of coolant - 16.4 MPa.
- Coolant flow rate - 84 000 m^3/h.
- Position of control rods regulating bank - 70% from the core bottom.
- Xe eq (Wnom) and Sm eq

5.3. *Scenario of transient*

Accident with steam line rupture in one of the loops between the steam generator and steam generator stop valve, with the power unit de-energized. Accident sequence is shown in Table 5.1.

Table 5-1. Accident sequence

Time, sec	Events and parameters
0.0	The reactor plant operates at Wnom; parameters of primary and secondary circuits are within the permissible limits with allowance for deviations.
0.3	The steam line is depressurized, in the period from 0.3s to 0.6s the rupture cross section increases linearly up to the full steam line cross section.
2.6	Scram is actuated (all rods except for the most effective). Duration of the rod drop is 4 sec.
20	BRUAs operate, the pressure in three intact SG is maintained within the rated limits.

These events lead to variations of core parameters that are shown in Table 5.2. The temperature values are calculated under assumption of the absence of coolant mixing between the loops. Assembly numbers in the one fourth part of the core connected with ruptured steam line are: 4-6, 11-15, 21-25, 31-36, 43-48, 55-61, 69-75, 82. Fig 5.1 shows the changes in the inlet temperature in the overcooled fourth part of the core and other assemblies.

Table 5-2. Variation of Core Parameters in the Accident with Steam Line Rupture and Power Unit de-Energized

Time. sec	Reactor coolant system parameters			
	t_{entry}, °C		Flow rate through the core. G/G_{nom}	Pressure, MPa
	$t_{1/4\ core}$	$t_{3/4\ core}$		
0	287	287	1	16.4
10	272	280	0.8	14.5
20	248	270	0.6	13.9
30	229	259	0.45	13.6
40	220	248	0.35	13.4
50	225	246	0.3	13.4

5.4. *Results of calculations.*

The calculation results of dynamical processes are shown in Figs. 5.1-5.7, Figs. 5.3-5.6 present the characteristics of «hot» channel with sampling all over the core. Fig. 5.7 presents the power of assembly number 24 located in the overcooled fourth part of the core, and power of assembly number 129.

The analysis of Figs. 5.1 – 5.7 shows that for the accident considered the MOX-zone proved to be more dangerous. However this difference is very small.

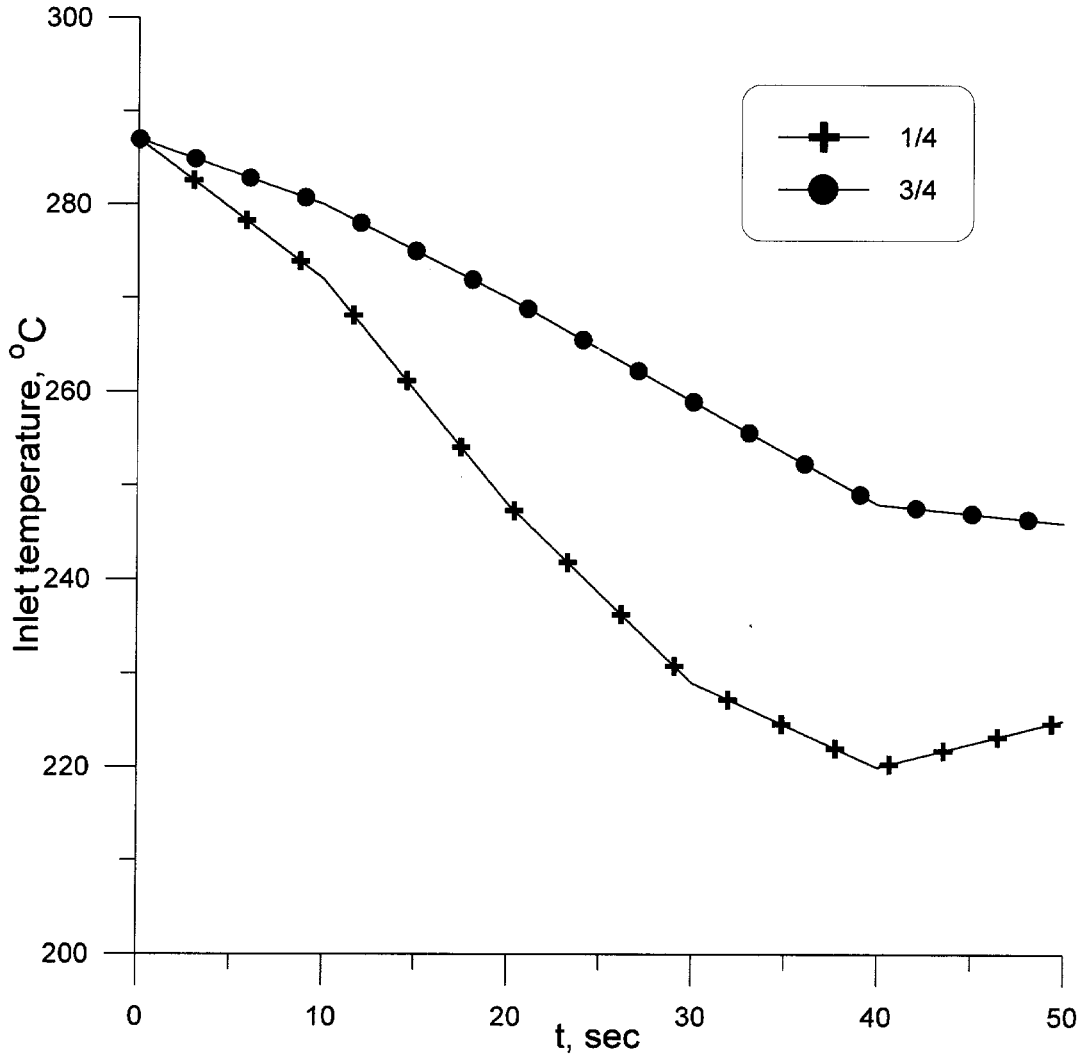

Fig. 5-1. Inlet Temperature in Different Parts of the Core. Partial Core Overcooling

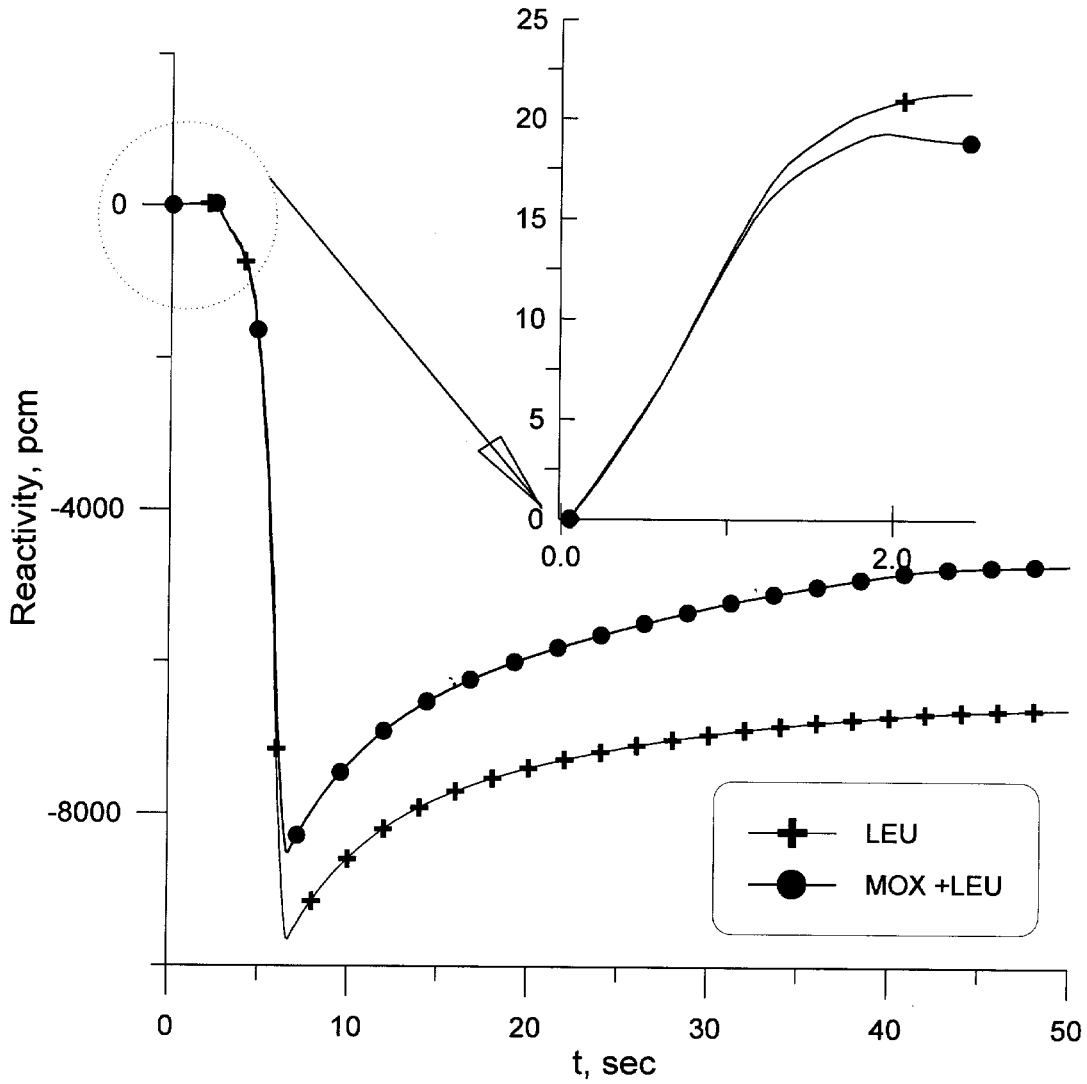

Fig. 5-2. Reactivity. Partial Core Overcooling

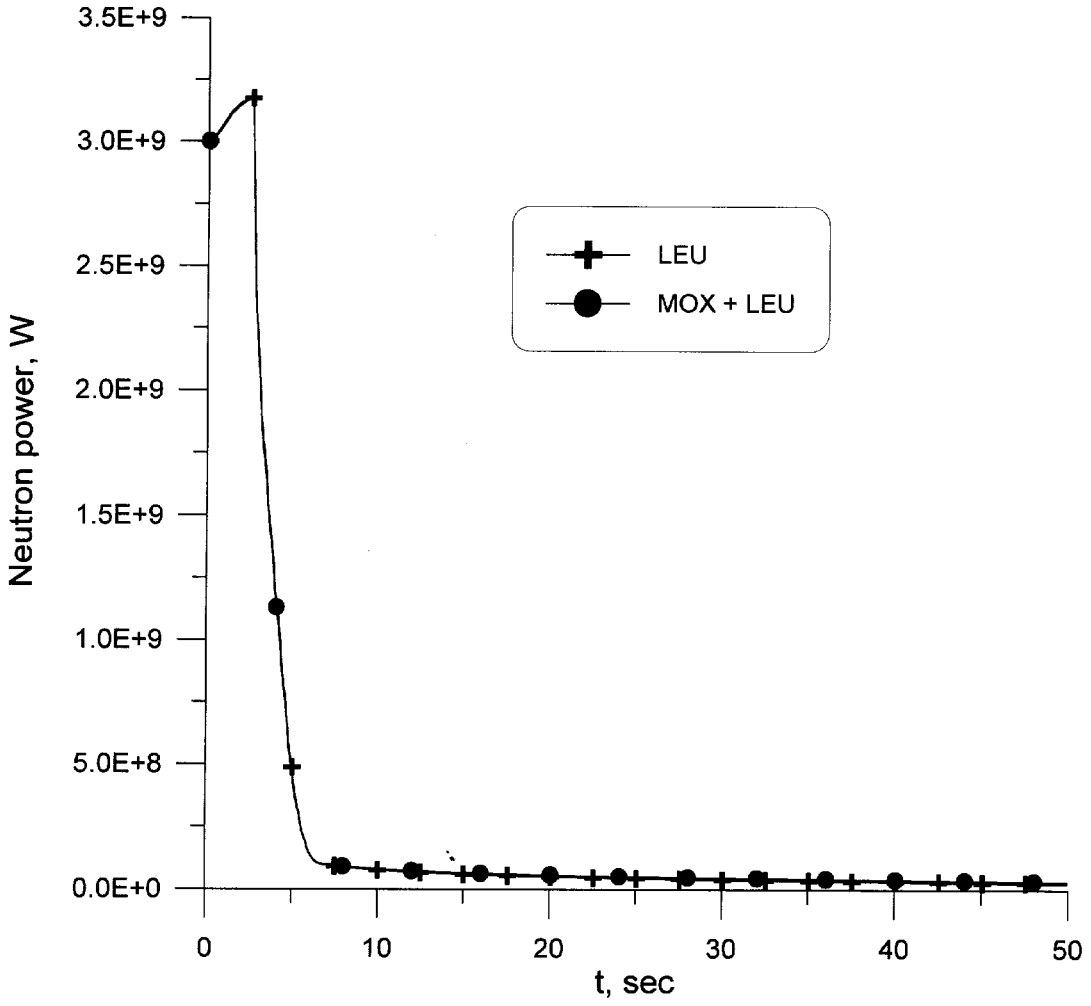

Fig. 5-3. Neutron Power. Partial Core Overcooling

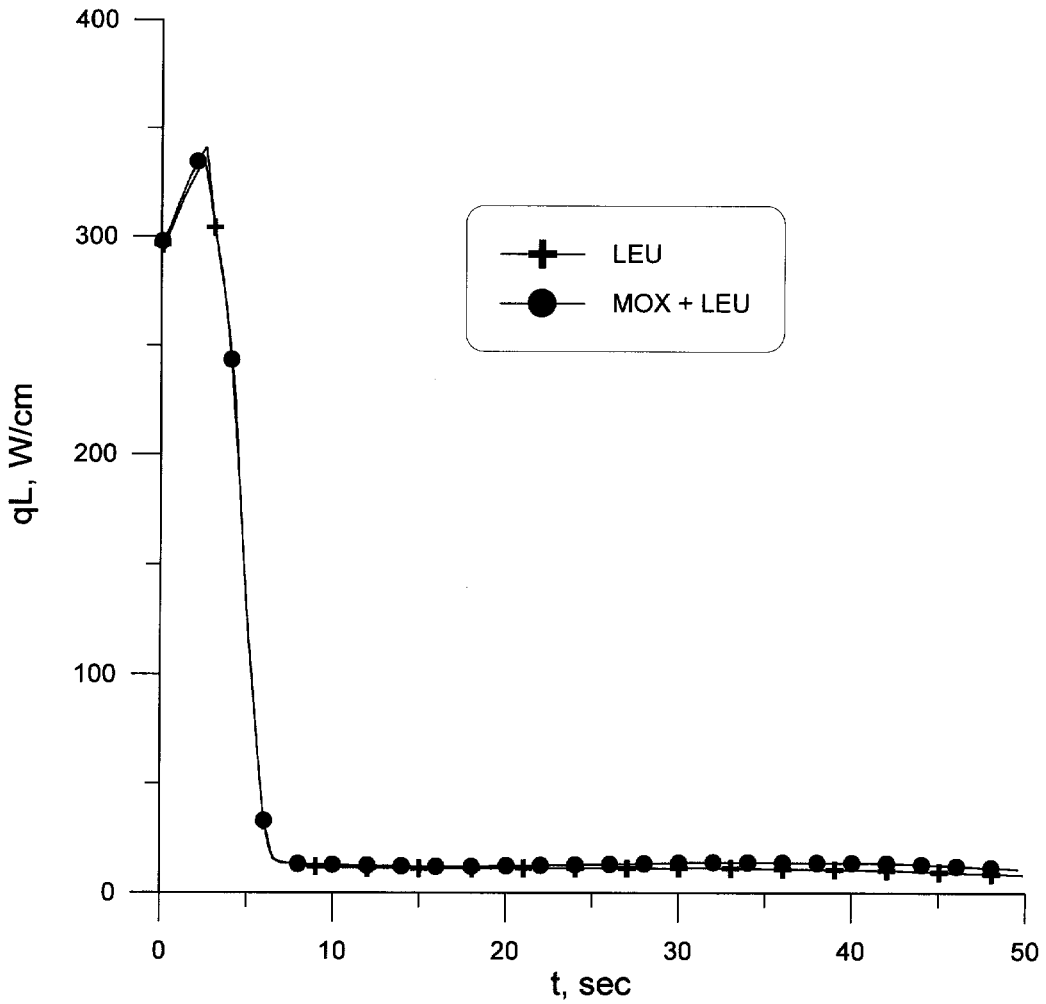

Fig. 5-4. Maximal Neutron Linear Power. Partial Core Overcooling

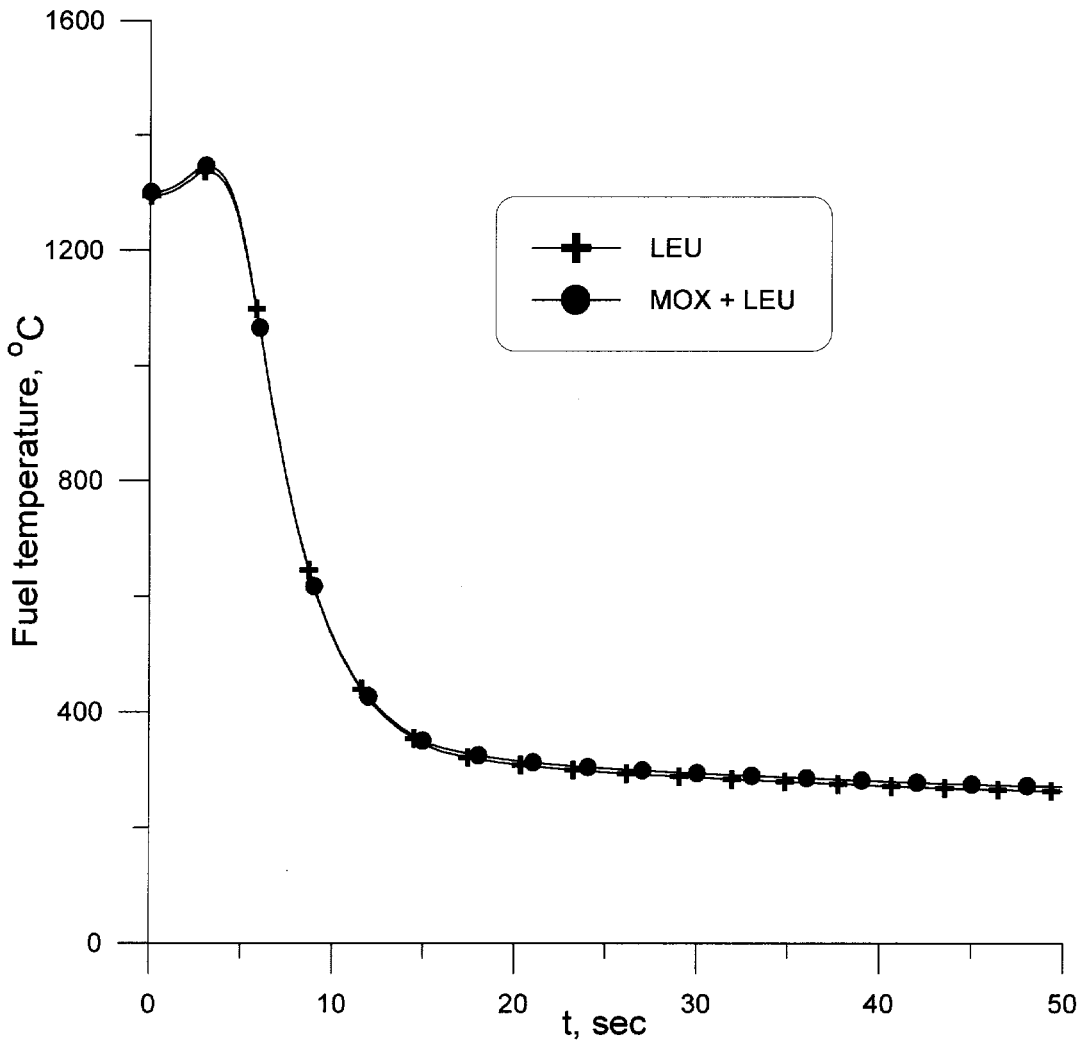

Fig. 5-5. Maximal Fuel Temperature. Partial Core Overcooling

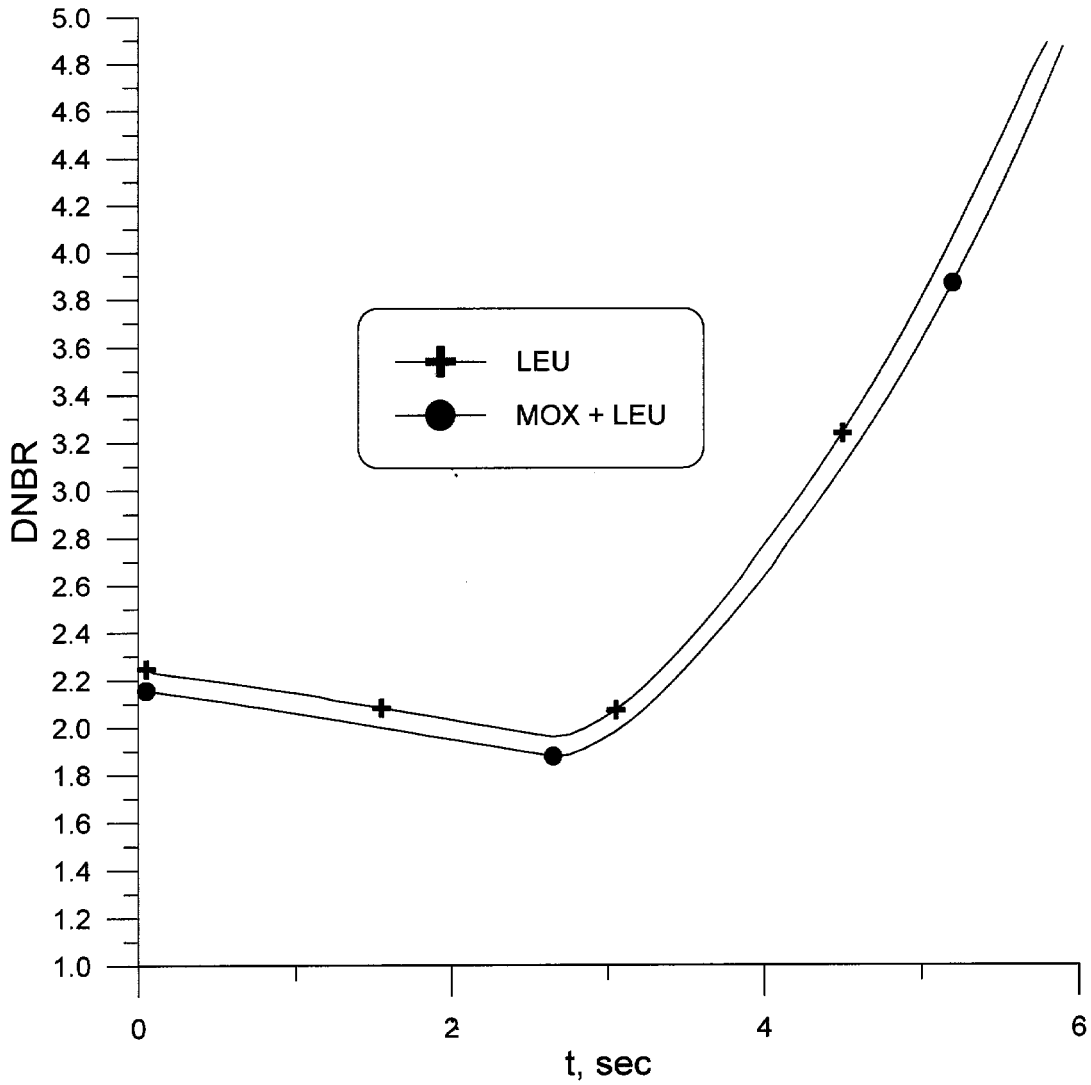

Fig. 5-6. Minimal DNBR. Partial Core Overcooling

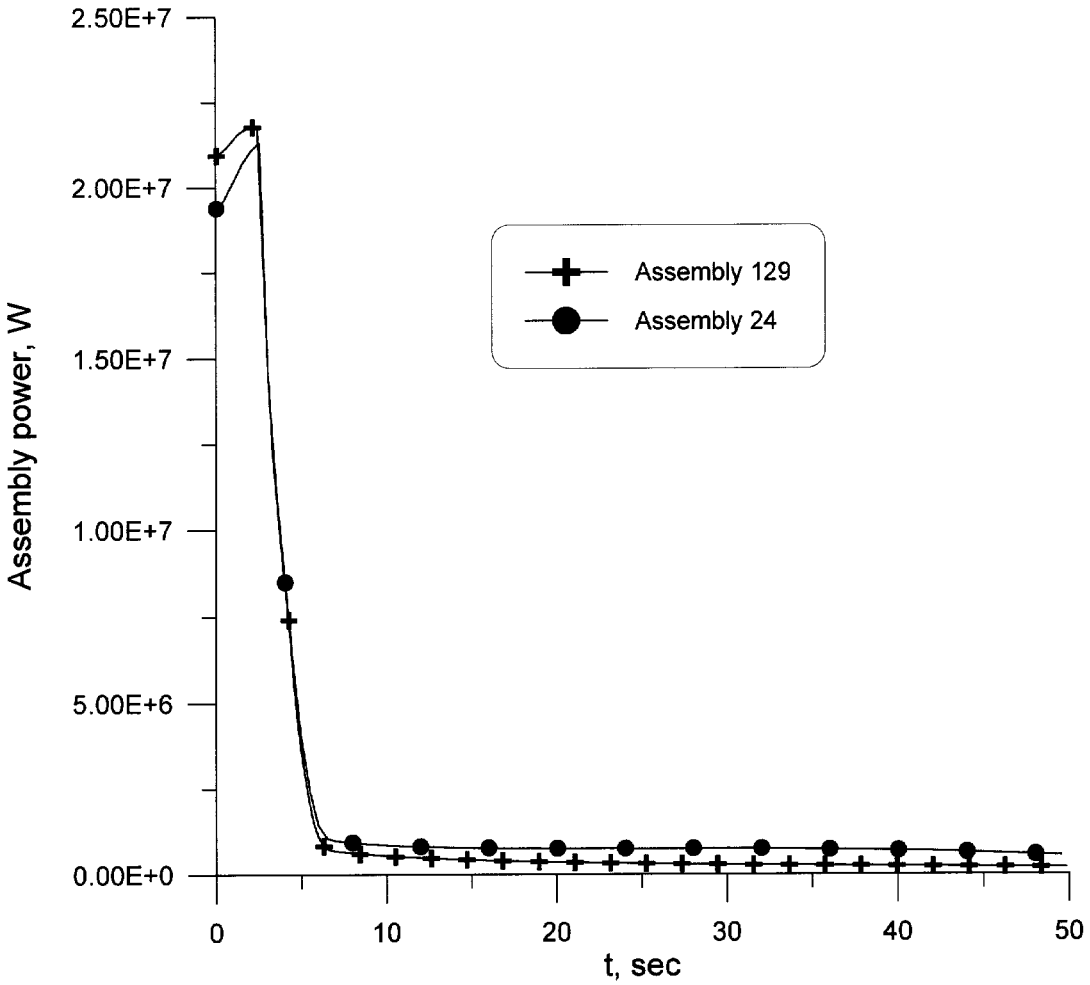

Fig. 5-7. Assembly Power. Partial Core Overcooling. MOX + LEU

6. The Boron Dilution of Coolant in a Part of the VVER-1000 Core

6.1 *Process being investigated*: The boron dilution of coolant in part of the VVER-1000 core caused by penetration of the distillate slug into the core at start up of non-working loop.

6.2. *Initial state of the core*:

- BOC for equilibrium refueling regime.
- W = 0.66 Wnom.
- Three main circulating pumps are working, coolant flow rate - 75% of nominal value 84 000 m^3/h.
- Position of control rods regulating bank - 80% from the core bottom.
- Xe eq (Wnom) and Sm eq.

6.3. *Scenario of transient.*

At initial time point (4.0 sec) the fourth main circulating pump is assumed to be switched on. The flow rate of this pump changes linearly during 30 sec from 0% to 100% of nominal value (21000 m^3/h).

At time point of 6.0 sec the distillate slug comes to the core inlet.

When the reactor power exceeds 110% of initial value, the scram activates. Duration of the rod drop is 4 sec.

Simultaneously with activation of the scram, the most effective control rod located in the cell 58 of the 5th bank is stuck at its upper position.

It is assumed that full amount of coolant from the activated loop comes into the one-fourth part of the core (see below Fig. 6-1).

Within this quarter of the core the distillate and coolant coming from other loops are fully mixed.

The boric acid concentration at inlet of this quarter C(t) changes according to the following dependence:

$$\begin{cases} C(t) = C_H; & t < \tau_1 \\ C(t) = \dfrac{3\left(1 - \dfrac{t}{\tau}\right)}{3 + \dfrac{t}{\tau}} C_H; & \tau_1 < t \le \tau \\ C(t) = 0.0; & t > \tau \end{cases}$$

where C_H - critical boric acid concentration for initial state;
τ_1 - time point when the distillate slug enters into the core (4 sec);
τ - end of startup period for the 4th pump (34 sec).

Concentration of boric acid in other 3/4 part of the core does not change during the transient.

6.4. *Main calculation results.*

Fig. 6-2 shows the change in the boric acid concentration in the typical fuel assembly of sector 1.

The calculation results of dynamical process are given in Figs. 6-3 - 6-9, Figs. 6-5 - 6-8 show the "hot" channel (sampling is made over the whole core).

As far as the neutron power is concerned, the first downward kink of the curve is accounted for by the drop of safety control rods, the second - for the Doppler effect.

The analysis of Figs. 6-3 – 6-9 shows that for the accident considered the MOX-zone proved to be more dangerous. However this difference is not very important. The short-time DNB both in LEU and MOX + LEU cores is possible.

Fig. 6-1. Numbers of Fuel Assemblies in the Quarter of the Core

82 83 84 85 86 87 88

69 70 71 72 73 74 75

55 56 57 58 59 60 61

43 44 45 46 47 48

32 33 34 35 36
21 22 23 24 25

12 13 14 15

4 5 6 Sector 1

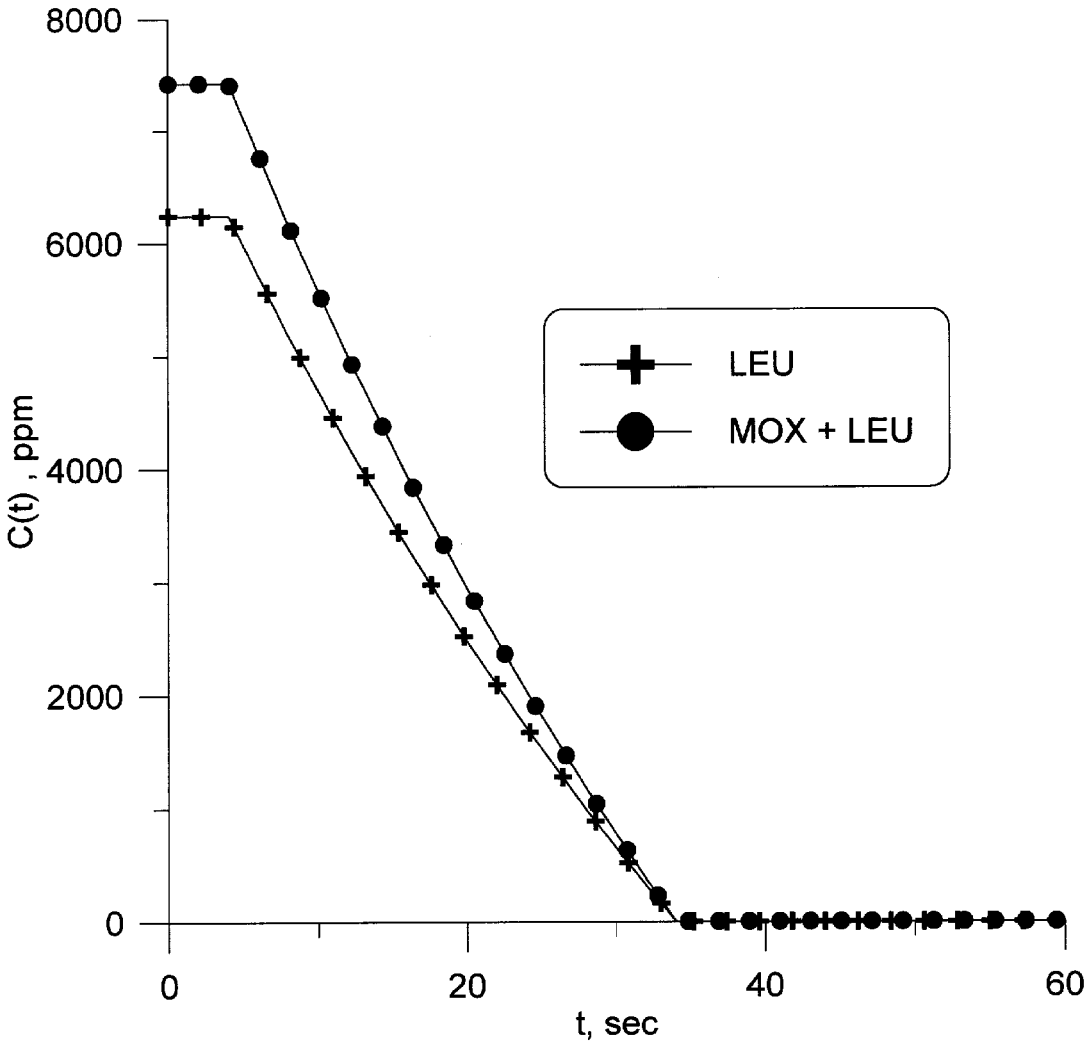

Fig. 6-2. Concentration of Boron Acid. Loop Put into Operation & Boron Dilution

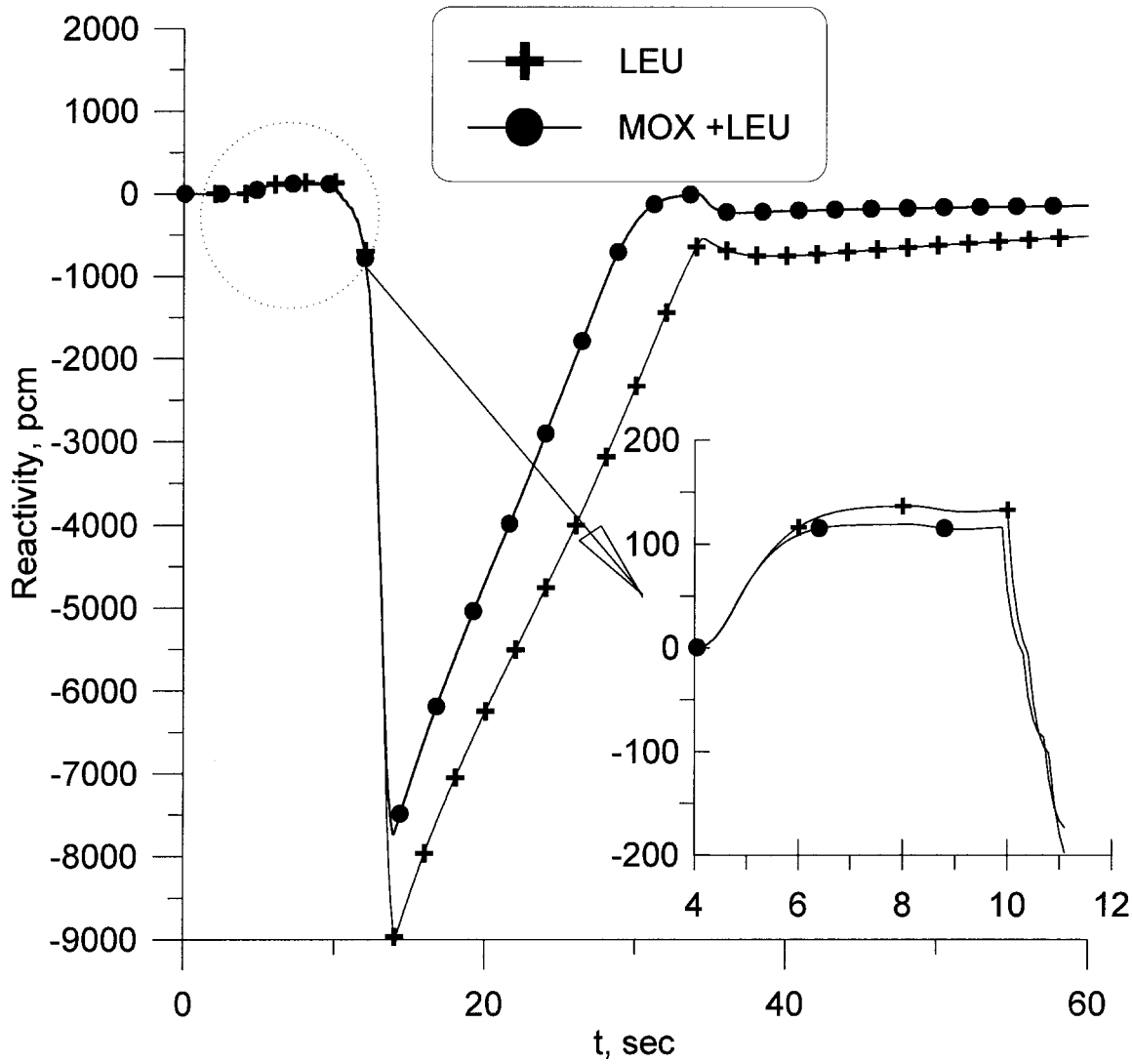

Fig. 6-3. Reactivity. Loop Put into Operation & Boron Dilution

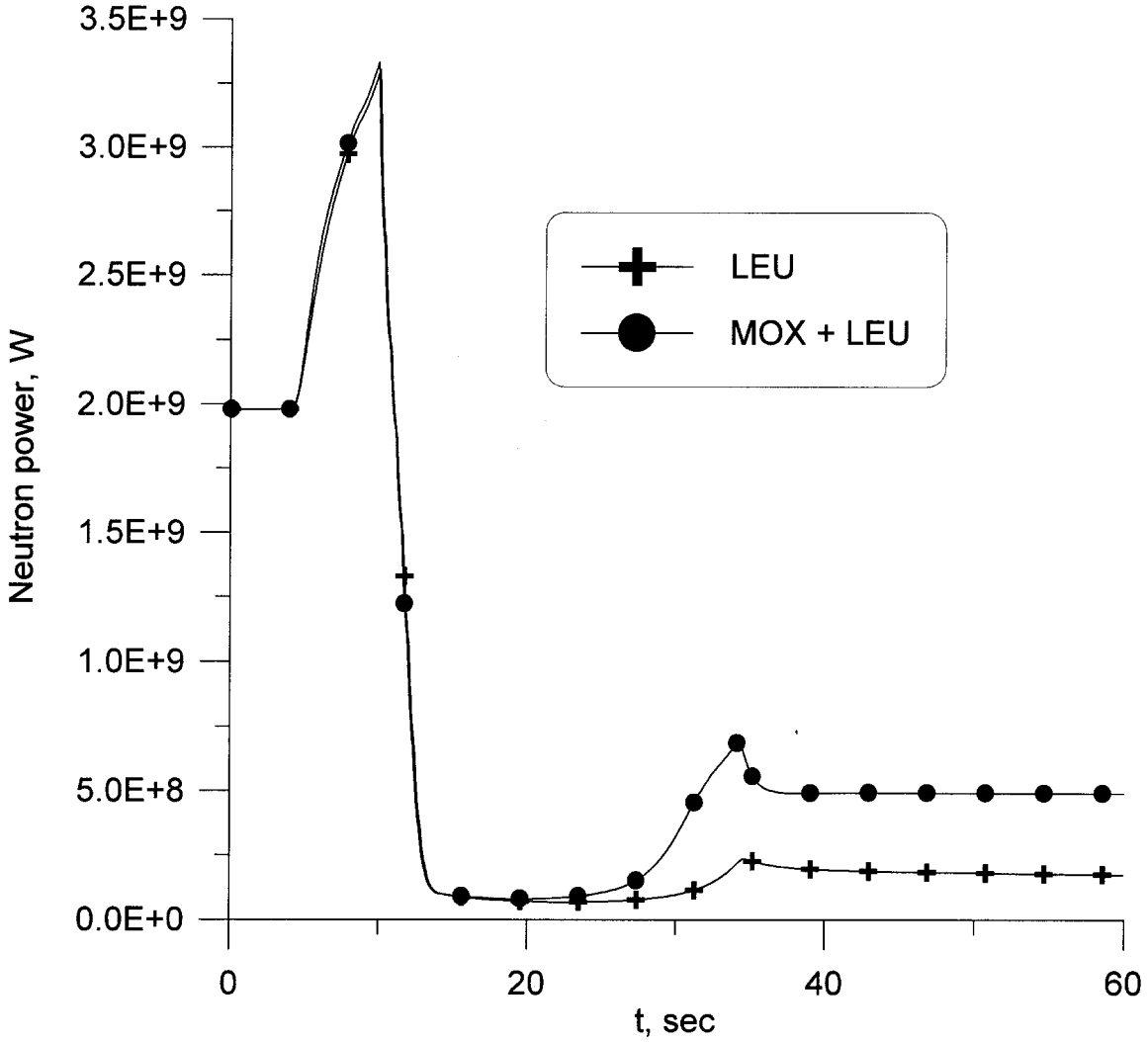

Fig. 6-4. Neutron Power. Loop Put into Operation & Boron Dilution

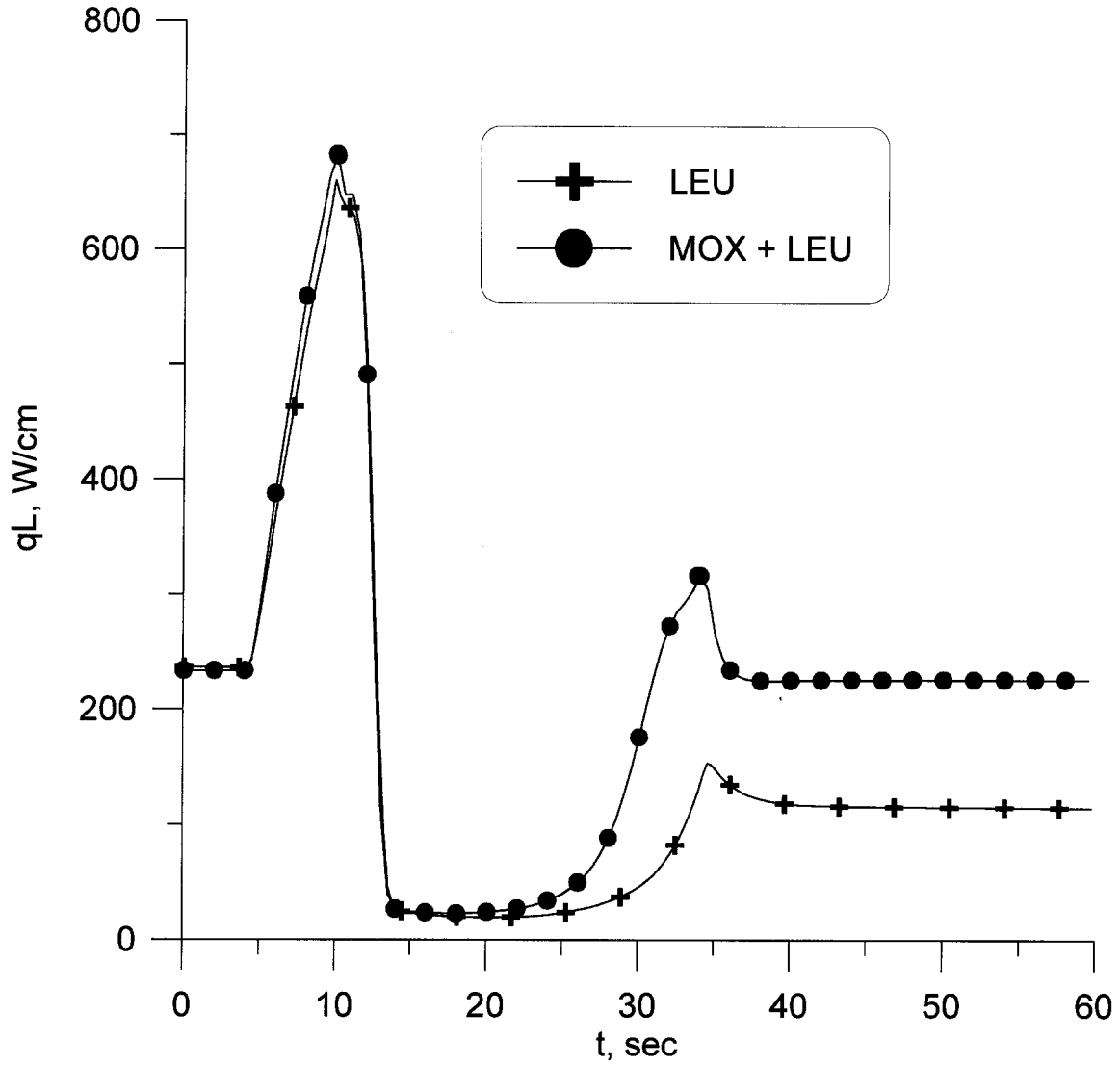

Fig. 6-5. Maximal Neutron Power. Loop Put into Operation & Boron Dilution

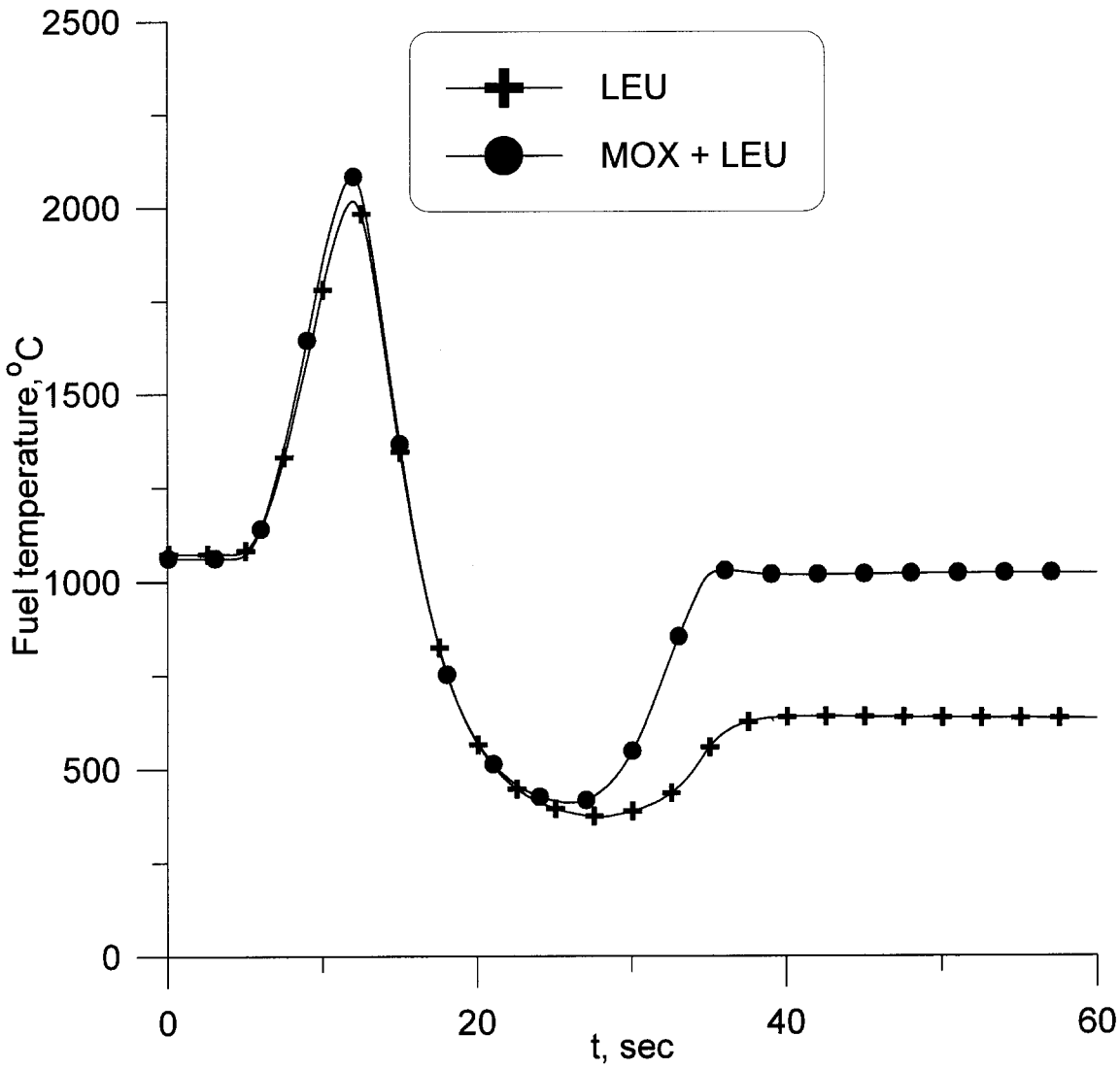

Fig. 6-6. Maximal Fuel Temperature. Loop Put into Operation & Boron Dilution

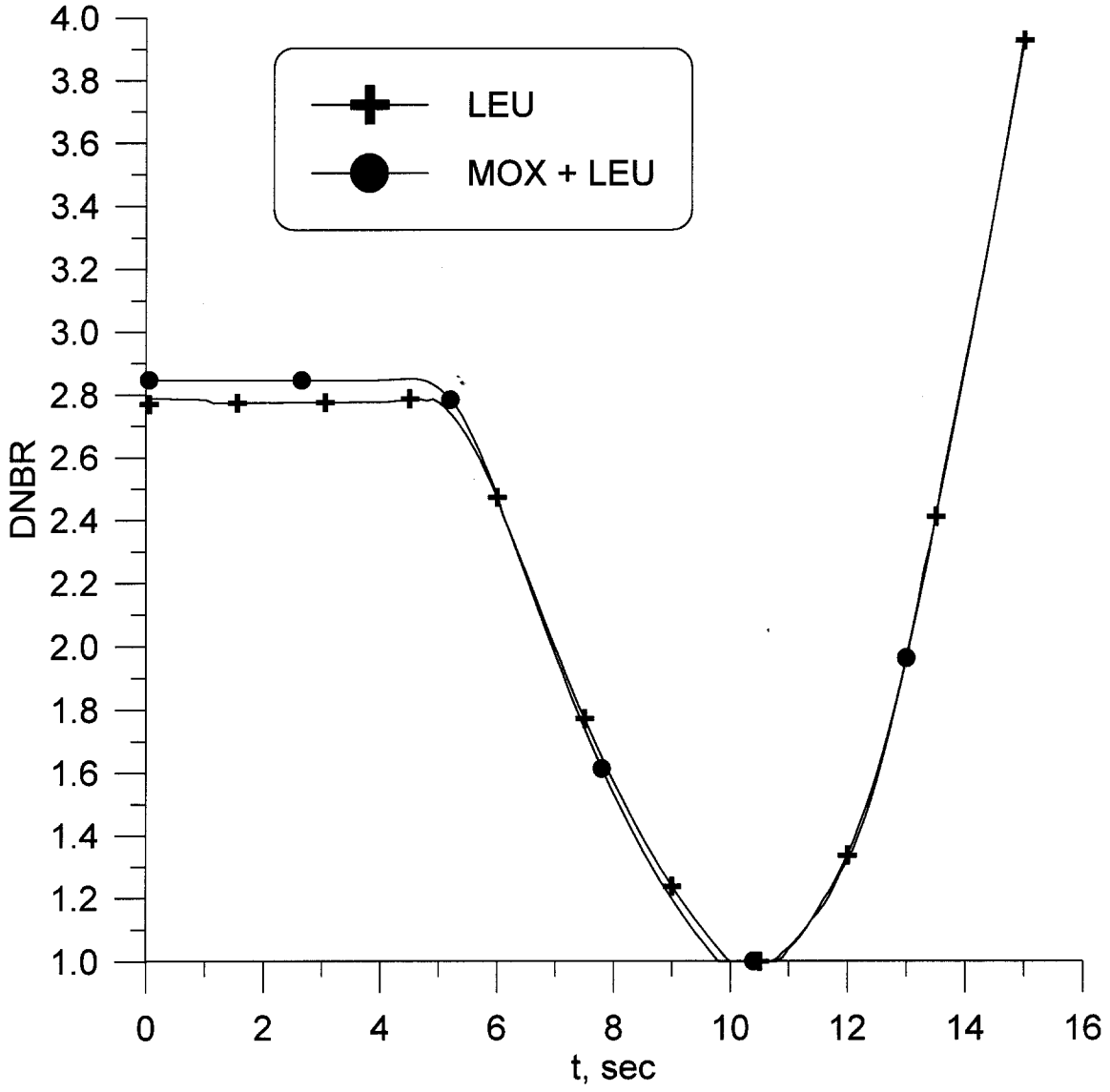

Fig. 6-7. Minimal DNBR. Loop Put into Operation & Boron Dilution

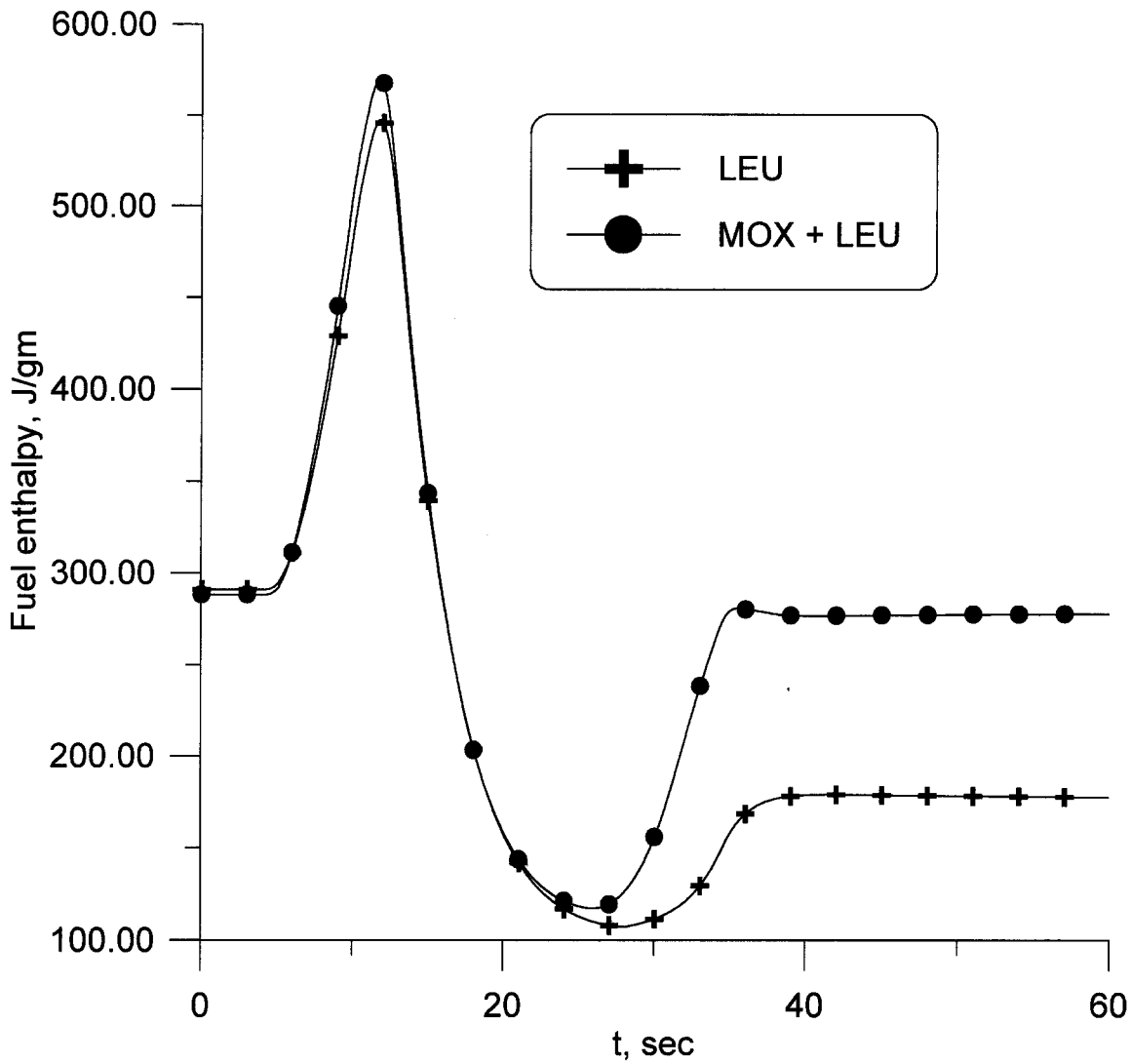

Fig. 6-8. Maximal Fuel Enthalpy. Loop Put into Operation & Boron Dilution

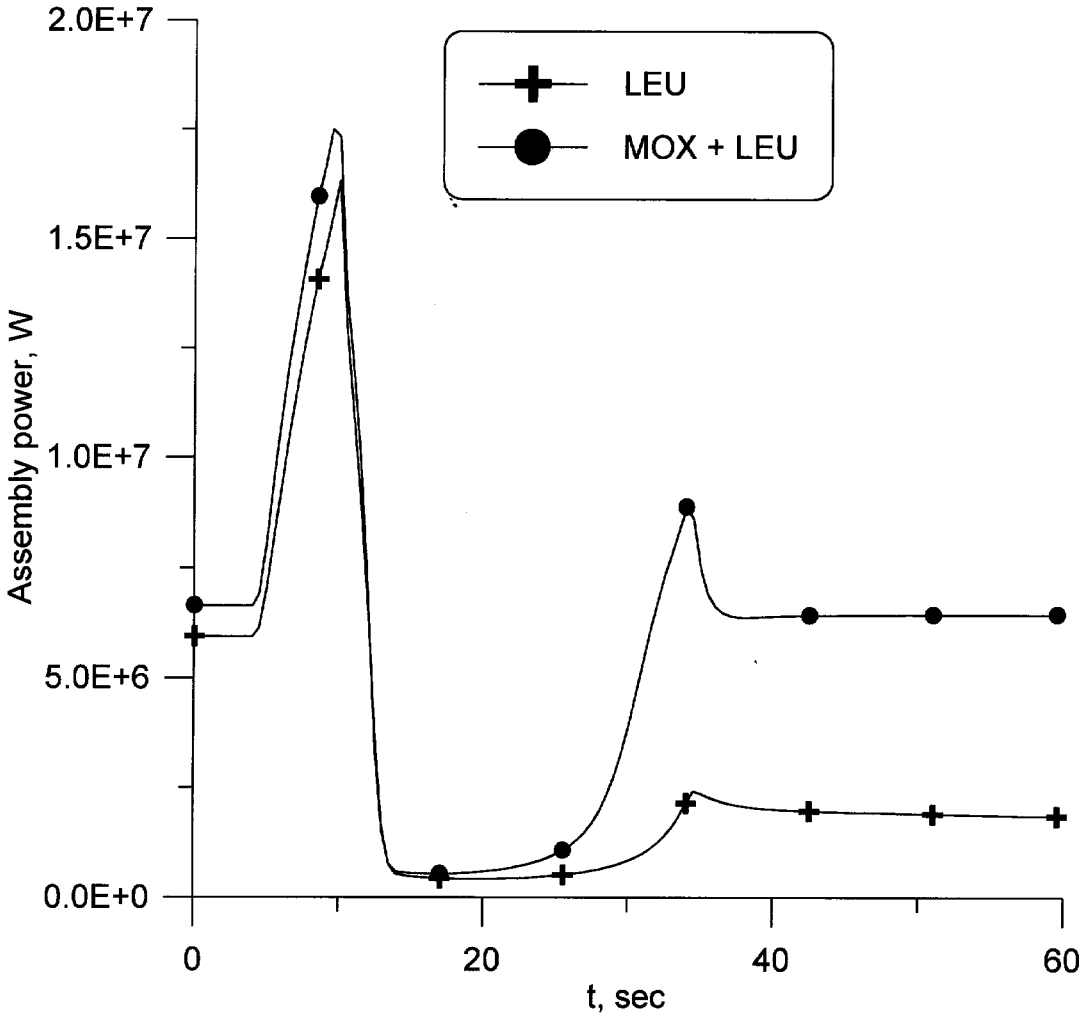

Fig. 6-9. Power of Assembly N 4. Loop Put into Operation & Boron Dilution

CONCLUSION

The analysis of results of the three dynamic problems solution allows to conclude, that their solution with the help of different codes will help to execute verification of codes, which one in further will be used for modelling of the transition and emergency modes of VVER operation.

These results obtained by 3D kinetics model of the Russian code NOSTRA can be used for comparison with a point kinetics model that is often used in accident analysis codes such as RELAP. In future the present analysis should be used for 3D model introduction in RELAP code.

REFERENCE

1. K.L.Nikitin et al. Verification of the three-dimensional dynamic code NOSTRA. Problems of nuclear power installation safety. These of paper presented to the IX Seminar on reactor physics problems. Moscow, MEPhI, 1995.
2. In-core fuel management code package validation for WWERs. IAEA-TECDOC-847. November 1995.

Comments from Oak Ridge National Laboratory staff on *Spatial Kinetics Calculations of MOX Fuelled Core: Variant 22*

1. The technical content of the report satisfies the milestone request from ORNL. When the MOX fuel assembly design is finalized and the final core loading pattern is selected, these calculations will be repeated for that design. At that time, it is expected that a final report for this effort will be generated, and we recommend that the Russian version as well as the English version of the final report be supplied to the United States so that the best possible translation from Russian to English is accomplished.

2. Chapter 2 is simply one big table with no text. If the report were to conform to ORNL standards, this table should either be combined with another chapter or additional text should be included referencing this table.

3. On page 15, the statement that the position of the regulating rod bank is 80% is interpreted to mean that the regulating rod bank is 80% inserted (see also comment on page 38).

4. On page 18, the MOX pin is stated to have a central hole diameter of 1.5 mm. Previously, there has been no commitment from Russia as to the presence or lack of a central hole in MOX pins.

5. On pages 33 and 34, a definition of "corner" and "plane" on these figures is lacking.

6. On page 48, the position of the regulating rod bank is specified as being 70% from the core bottom. This is assumed to be a typical end-of-cycle value.

7. On page 57, the equation describing the boron concentration in the time interval $\tau_1 < t < \tau$ is not correct in that it does not account for the τ_1 time offset. The correct equation probably should be:

$$C(t) = \frac{3\left(1 - \frac{(t-\tau_1)}{(\tau-\tau_1)}\right)}{3 + \frac{(t-\tau_1)}{(\tau-\tau_1)}}$$

8. For future reference, if revisions of these calculations are to be used for verification purposes, the detailed results of all parameters of interest should be given in tabular form in appendixes to allow for easier comparison of results.

INTERNAL DISTRIBUTION

1. R. J. Belles
2–6. B. B. Bevard
7. J. J. Carbajo
8. M. D. DeHart
9. F. C. Difilippo
10. R. J. Ellis
11. S. E. Fisher
12–16. J. C. Gehin
17. S. R. Greene
18. R. Holdaway
19. D. T. Ingersoll
20. M. A. Kuliasha
21. S. B. Ludwig
22. M. G. McGinnis
23. G. E. Michaels
24. D. L. Moses
25. W. P. Poore
26–30. R. T. Primm III
31. C. C. Southmayd
32. D. J. Spellman
33. G. L. Yoder, Jr.
34. Central Research Library
35–36. ORNL Laboratory Records (OSTI)
37. ORNL Laboratory Records (RC)

EXTERNAL DISTRIBUTION

38. M. L. Adams, Department of Nuclear Engineering, Texas A&M University, Zachry 129, College Station, TX 77843
39. D. Alberstein, Los Alamos National Laboratory, MS-K551, P.O. Box 1663, Los Alamos, NM 87545
40. Dr. Kiyonori Aratani, Surplus Weapons Plutonium Disposition Group; International Cooperation and Nuclear Material Control Division; Japan Nuclear Cycle Development Institute; 4-49 Muramatsu, Tokai-mura, Naka-gun, Ibaraki-ken, Japan
41. J. Baker, Office of Fissile Materials Disposition, U.S. Department of Energy, MD-3, 1000 Independence Avenue SW, Washington, DC 20585
42. M. S. Chatterton, Office of Nuclear Reactor Regulation, MS O10B3, U.S. Nuclear Regulatory Commission, Washington, DC 20555-0001
43. K. Chidester, Los Alamos National Laboratory, MS-E502, P.O. Box 1663, Los Alamos, NM 87545
44. R. H. Clark, Duke/Cogema/Stone & Webster, 400 South Tryon Street, WC-32G, P.O. Box 1004, Charlotte, NC 28202
45. W. Danker, U.S. Department of Energy, MD-3, 1000 Independence Avenue SW, Washington DC 20585
46. N. Fletcher, Office of Fissile Materials Disposition, U.S. Department of Energy, MD-3, 1000 Independence Avenue SW, Washington DC 20585
47. T. Gould, Lawrence Livermore National Laboratory, P.O. Box 808, MS-L186, Livermore, CA 94551
48. L. Holgate, Office of Fissile Materials Disposition, U.S. Department of Energy, MD-1/2, 1000 Independence Avenue SW, Washington DC 20585
49. L. Jardine, Lawrence Livermore National Laboratory, P.O. Box 808, MS-L166, Livermore, CA 94551

50. Dr. Alexander Kalashnikov, Institute of Physics and Power Engineering, 1 Bondarenko Square, Obninsk, Kaluga Region, Russia 249020

51–55. D. E. Klein, Associate Vice Chancellor for Special Engineering Programs, The University of Texas System, 210 West Sixth Street, Austin, TX 78701

56. R. W. Lee, Office of Nuclear Reactor Regulation, MS O10B3, U.S. Nuclear Regulatory Commission, Washington, DC 20555-0001

57. S. Nesbit, Duke/Cogema/Stone & Webster, 400 South Tryon Street, WC-32G, P.O. Box 1004, Charlotte, NC 28202

58. J. O. Nulton, Office of Fissile Materials Disposition, U.S. Department of Energy, MD-3, 1000 Independence Avenue SW, Washington, DC 20585

59. Nagao Ogawa; Director and General Manager; Plant Engineering Department; Nuclear Power Engineering Corporation; Shuwa-Kamiyacho Building, 2F; 3-13, 4-Chome Toranomon; Minato-Ku, Tokyo 105-0001, Japan

60. Dr. S. L. Passman, Booz-Allen & Hamilton, 555 13th Street, NW, No. 480E, Washington, DC 20004

61–65. Dr. Alexander Pavlovitchev, Russian Research Center “Kurchatov Institute,” Institute of Nuclear Reactors, VVER Division, VVER Physics Department, 123182, Kurchatov Square, 1, Moscow, Russia

66. K. L. Peddicord, Associate Vice Chancellor, Texas A&M University, 120 Zachry, College Station, TX 77843-3133

67. W. D. Reece, Texas A&M University, Department of Nuclear Engineering, Zachry 129, College Station, TX 77843-3133

68. P. T. Rhoads, Office of Fissile Materials Disposition, U.S. Department of Energy, MD-4, 1000 Independence Avenue SW, Washington, DC 20585

69. U. Shoop, Office of Nuclear Reactor Regulation, MS O10B3, United States Nuclear Regulatory Commission, Washington, DC 20555-0001

70. J. Thompson, Office of Fissile Materials Disposition, U.S. Department of Energy, MD-4, 1000 Independence Avenue SW, Washington, DC 20585

71. F. Trumble, Westinghouse Savannah River Company, Building 730R, Room 3402, WSRC, Aiken, SC 29808

72. Dr. Boris E. Volkov; Head of Division; EDO Gidropress, 21 Ordzhonikidze Street, Podolsk, Moscow District, Russia 142103